Am J Physiol Cell Physiol 317: C287–C302, 2019.
First published May 15, 2019; doi:10.1152/ajpcell.00074.2019.

RESEARCH ARTICLE

Erythrocyte ion content and dehydration modulate maximal Gardos channel activity in KCNN4 V282M/+ hereditary xerocytosis red cells

Alicia Rivera,[1] David H. Vandorpe,[1] Boris E. Shmukler,[1] Immacolata Andolfo,[2] Achille Iolascon,[2] Natasha M. Archer,[3] Estela Shabani,[4] Michael Auerbach,[5] Nelson Hamerschlak,[6] James Morton,[7] Jay G. Wohlgemuth,[7] Carlo Brugnara,[8] L. Michael Snyder,[9,10]* and Seth L. Alper[1,11]*

[1]*Department of Medicine, Beth Israel Deaconess Medical Center and Harvard Medical School, Boston, Massachusetts;* [2]*Department of Molecular Medicine and Medical Biotechnologies, "Federico II" University of Naples, CEINGE Biotecnologie Avanzate, Naples, Italy;* [3]*Division of Hematology and Oncology, Boston Children's Hospital, Dana-Farber Cancer Center, Department of Pediatrics, Harvard Medical School, Boston, Massachusetts;* [4]*Department of Immunology and Infectious Diseases, Harvard T. H. Chan School of Public Health, Boston, Massachusetts;* [5]*Auerbach Hematology-Oncology, Rosedale, Maryland;* [6]*Department of Hematology, Hospital Israelita Albert Einstein, Sao Paulo, Brazil;* [7]*Quest Diagnostics, San Juan Capistrano, California;* [8]*Department of Laboratory Medicine, Boston Children's Hospital and Department of Pathology, Harvard Medical School, Boston, Massachusetts;* [9]*Quest Diagnostics, Marlborough, Massachusetts;* [10]*Departments of Medicine and Laboratory Medicine, University of Massachusetts Medical Center, Worcester, Massachusetts; and* [11]*Broad Institute of Harvard and Massachusetts Institute of Technology, Cambridge, Massachusetts*

Submitted 28 February 2019; accepted in final form 14 May 2019

Rivera A, Vandorpe DH, Shmukler BE, Andolfo I, Iolascon A, Archer NM, Shabani E, Auerbach M, Hamerschlak N, Morton J, Wohlgemuth JG, Brugnara C, Snyder LM, Alper SL. Erythrocyte ion content and dehydration modulate maximal Gardos channel activity in KCNN4 V282M/+ hereditary xerocytosis red cells. *Am J Physiol Cell Physiol* 317: C287–C302, 2019. First published May 15, 2019; doi:10.1152/ajpcell.00074.2019.—Hereditary xerocytosis (HX) is caused by missense mutations in either the mechanosensitive cation channel PIEZO1 or the Ca^{2+}-activated K^+ channel KCNN4. All HX-associated KCNN4 mutants studied to date have revealed increased current magnitude and red cell dehydration. Baseline KCNN4 activity was increased in HX red cells heterozygous for KCNN4 mutant V282M. However, HX red cells maximally stimulated by Ca^{2+} ionophore A23187 or by PMCA Ca^{2+}-ATPase inhibitor orthovanadate displayed paradoxically reduced KCNN4 activity. This reduced Ca^{2+}-stimulated mutant KCNN4 activity in HX red cells was associated with unchanged sensitivity to KCNN4 inhibitor senicapoc and KCNN4 activator Ca^{2+}, with slightly elevated Ca^{2+} uptake and reduced PMCA activity, and with decreased KCNN4 activation by calpain inhibitor PD150606. The altered intracellular monovalent cation content of HX red cells prompted experimental nystatin manipulation of red cell Na and K contents. Nystatin-mediated reduction of intracellular K^+ with corresponding increase in intracellular Na^+ in wild-type cells to mimic conditions of HX greatly suppressed vanadate-stimulated and A23187-stimulated KCNN4 activity in those wild-type cells. However, conferral of wild-type cation contents on HX red cells failed to restore wild-type-stimulated KCNN4 activity to those HX cells. The phenotype of reduced, maximally stimulated KCNN4 activity was shared by HX erythrocytes expressing heterozygous PIEZO1 mutants R2488Q and V598M, but not by HX erythrocytes expressing heterozygous KCNN4 mutant R352H or PIEZO1 mutant R2456H. Our data suggest that chronic KCNN4-driven red cell dehydration and intracellular cation imbalance can lead to reduced KCNN4 activity in HX and wild-type red cells.

dehydrated stomatocytosis; ionophore; potassium channel; red blood cell; senicapoc

INTRODUCTION

Hereditary xerocytosis (HX; also known as dehydrated hereditary stomatocytosis) is an autosomal dominant hemolytic anemia caused by heterozygous mutations in either of two genes, the mechanosensitive cation channel *PIEZO1* (1, 3, 60) and the intermediate conductance calcium-activated K^+ channel *KCNN4* (5, 41). The clinical and molecular characteristics of HX patients were recently summarized in two large clinical series (4, 6, 15, 39). HX can manifest as moderate to debilitating fatigue and with frank or fully compensated hemolytic anemia accompanied by variable splenomegaly, hyperbilirubinemia and jaundice, gallstones, transient perinatal edema, pseudohyperkalemia, and systemic iron overload disproportionate to the degree of hemolysis and transfusion frequency. Splenectomy has been associated with a hyperthrombotic state in mutant PIEZO1-associated HX, but this association has not yet been reported among previously splenectomized mutant KCNN4-associated HX patients. HX patients can show considerable cellular and clinical phenotypic variability within individual families, as well as among different families carrying the same or different mutations (4, 6, 15, 39).

HX-associated mutations in both *PIEZO1* and *KCNN4* have been characterized functionally as gain-of-function mutations (1, 3, 5, 8, 22, 41). HX-associated PIEZO1 mutant polypeptides expressed in human embryonic kidney (HEK)-293 cells generally exhibited delayed inactivation kinetics proposed to increase Ca^{2+} entry and elevate intracellular [Ca^{2+}] (14, 33), leading in turn to hyperactivation of erythroid KCNN4. HX-associated KCNN4 mutant polypeptides studied in HEK-293 cells and in patient red cells generally exhibited increased current magnitude in the presence of intracellular Ca^{2+} (42,

* L. M. Snyder and S. L. Alper contributed equally to this work.
Address for reprint requests and other correspondence: S. L. Alper, Beth Israel Deaconess Medical Center, RN380F, 99 Brookline Ave., Boston, MA 02215 (e-mail: salper@bidmc.harvard.edu).

44). More recent studies of HX-associated PIEZO1 polypeptides expressed in HEK-293 cells, however, have revealed a range of functional phenotypes, including some mutants that expressed paradoxically reduced function or reduced sensitivity to particular cellular deformations (22).

Reported HX-associated KCNN4 mutations include R352H located in the calmodulin-binding domain within the long COOH-terminal cytoplasmic tail, V282M and V282E in the transmembrane domain (5, 21, 41), and transmembrane domain mutants P204R and A279T reported in abstract (56).

Carriers of the KCNN4 V282M mutation were previously shown (4, 6, 15) to exhibit hemolytic anemia with occasional stomatocytes, increased resistance to osmotic lysis, increased cell density, reduced cell K content with elevated cell Na content, and a dramatically left-shifted ektacytometry curve with reduced D_{max} and O_{hyp} values indicative of decreased shear-sensitive deformability consistent with severe cell dehydration. V282M red cells were also shown to exhibit elevated baseline NPo sensitive to the inhibitor senicapoc, along with elevated, senicapoc-sensitive baseline influx of $^{86}Rb^+$, and elevated net K^+ efflux (41, 42, 44). KCNN4 residue V282 is of particular interest, as its isopropyl side chains within each homotetrameric KCNN4 channel together form the narrowest constriction of the KCNN4 inner pore (28). Whereas recombinant HX mutant V282E exhibited reduced sensitivity to the KCNN4 inhibitor senicapoc, recombinant mutant V282M preserved wild type (WT) senicapoc sensitivity (42).

The upstream action of PIEZO1-mediated elevation of intracellular $[Ca^{2+}]$ on KCNN4 in red cells, together with retention of sensitivity to senicapoc inhibition by some HX-associated KCNN4 mutant polypeptides, suggested that senicapoc might be an effective treatment for the gain-of-function phenotypes associated with both PIEZO1 and KCNN4 mutants (41, 42, 44). In preparation for a clinical trial of senicapoc treatment of HX in a family carrying the KCNN4 V282M mutation (5), we have more extensively characterized the properties of HX red cells from additional members of the same family, relying primarily on measurement of $^{86}Rb^+$ influx as a medium-throughput assay of KCNN4 activity.

Although we reproduced the earlier reported gain-of-function phenotypes in unstimulated HX V282M red cells, we were surprised to find apparent loss-of-function phenotypes in HX V282M red cells subjected to elevation of intracellular $[Ca^{2+}]$ through in vitro exposure to either the Ca^{2+} ionophore A23187 or the PMCA plasmalemmal Ca^{2+}-ATPase inhibitor orthovanadate. Therefore, we set out to describe the loss-of-function phenotypes in greater detail and compare them with the originally reported gain-of-function phenotypes.

METHODS

Drugs and chemicals. Senicapoc was from Pfizer (Cambridge, MA). A23187 was from Calbiochem (La Jolla, CA). $^{86}RbCl$ and $^{45}CaCl_2$ were from PerkinElmer Life Sciences (Boston, MA). BAPTA-AM and calpain inhibitor PD150606 were from Tocris (R & D Systems, Minneapolis, MN). All other reagents were from Sigma-Aldrich (St. Louis, MO).

Blood samples. Human blood samples were obtained with written informed consent from six hereditary xerocytosis (HX) patients from a previously described family expressing the heterozygous mutation KCNN4 V282M (5) and from six unrelated healthy control (unaffected) subjects. Blood collected in EDTA-containing Vacutainer tubes was transported by courier from collection centers to Boston Children's Hospital or to Beth Israel Deaconess Medical Center. All procedures were HIPAA-compliant and approved by the Institutional Review Boards of Boston Children's Hospital and Beth Israel Deaconess Medical Center. Data in each figure or table derive from the indicated number of HX subjects and from two to four unaffected individuals.

ADVIA hematological parameters. Whole blood hematological indices were determined by ADVIA 2120 Hematology Analyzer (Siemens Diagnostic Solutions, Tarrytown, NY), as previously described (17, 19, 40, 45). Whole blood was centrifuged 10 min at 1,500 *g*. Plasma was collected and stored at −90°C for subsequent study.

Erythrocyte KCNN4-mediated changes in hematological indices in baseline and activated states. Whole blood was partially leukodepleted by filtering through cotton and then centrifuged for 4 min at 4°C 1,500 *g* (Sorvall Legend RT; Thermo Scientific, Asheville, NC). Erythrocytes were washed five times with choline wash solution (CWS) containing (in mM) 150 choline Cl, 1 $MgCl_2$, and 10 Tris-MOPS at pH 7.4 (4°C) and stored at 4°C until use (generally within 18–24 h, always within 72 h). Washed erythrocytes were resuspended in 3% hematocrit in flux medium [normal saline containing (in mM) 2 KCl, 148 NaCl, 0.15 $MgCl_2$, 10 glucose, and 10 Tris-MOPS at pH 7.4 with either 1.5 or 0.1 $CaCl_2$]. Ouabain (0.1 mM) and bumetanide (1 mM) were added to incubation media at *time zero*. Erythrocyte KCNN4 was activated by addition to cell suspensions of either 5μM A23187 in the presence of 100 μM $CaCl_2$ or by the addition of 1 mM sodium orthovanadate (VO_3) in the presence of 1.5 mM $CaCl_2$. Time-dependent ADVIA hematological indices were determined in the absence or presence of 200 nM senicapoc (SCP).

Ektacytometry. Ektacytometry at constant osmolarity was perfomed at 37°C on the RheoScan-D Plus (RheoMeditech, Seoul, South Korea) at default settings.

Intracellular cation content. Intracellular contents of Na and K were determined in freshly isolated erythrocytes by atomic absorption spectrophotometry (AAnalyst 800; PerkinElmer, Norwalk, CT) as described (44, 45). Erythrocytes washed five times in CWS-Mg were suspended at 50% hematocrit in CWS-Mg, and an aliquot was used for manual determination of hematocrit. Lysates of suspensions diluted 1:50 (for cell Na determination) and 1:500 (for cell K determination) were prepared in 0.02% acationox, clarified by centrifugation at 3,000 rpm, and stored at 4°C for later atomic absorption spectrophotometry.

^{86}Rb influx in WT (V282) and HX (V282M) erythrocytes. Measurement of $^{86}Rb^+$ influx (a surrogate for K^+ influx) was performed in freshly washed erythrocytes. Cells were suspended at 3% hematocrit in normal saline influx media containing (in mM) 148 NaCl, 2 KCl, 0.15 $MgCl_2$, 0.1 ouabain, 10 Tris-MOPS pH 7.4 (22°C or 37°C as noted), 1.0 bumetanide, and 10 μCi/ml $^{86}RbCl$ in the presence or absence of 200 nM senicapoc (diluted from 50 μM DMSO stock). Measurements of $^{86}Rb^+$ influx at baseline conditions or in the presence of 1 mM sodium orthovanadate were performed in media containing 1.5 mM $CaCl_2$. Samples were preincubated in the absence or presence of orthovanadate for 30 min before the addition of isotope. Baseline and orthovanadate-stimulated $^{86}Rb^+$ fluxes were measured at 37°C or at room temperature in the absence of A23187 during the period 2–10 min following isotope addition. Measurements of $^{86}Rb^+$ influx activated by 5 μM A23187 were performed in media containing 100 μM $CaCl_2$. Fluxes were measured at 37°C or room temperature (as noted) during the period 2–6 min following isotope addition. Aliquots of cell suspension (100 μl) were removed and immediately microcentrifuged through 0.8 ml of ice-cold saline containing 5 mM EGTA resting on a 300-μl undercushion of *N*-butyl phthalate. After aspiration of both supernatant layers, tube tips containing cell pellets were cut off, and erythrocyte-associated ^{86}Rb was counted in a γ-counter (model 41600 HE; Isomedic ICN Biomedicals, Costa Mesa, CA). Ion fluxes were calculated from linear regression slopes. KCNN4 Ca^{2+} activation curves were performed by buffering extra-

cellular free Ca^{2+} from (nominal) 0 to 7 μM with either 1 mM EGTA or 1 mM citrate buffer at pH 7.4 in the presence of A23187 (5 μM) as described (43). Free [Ca^{2+}] was calculated from citrate or EGTA dissociation constants, correcting for ionic strength in the presence of 0.15 mM $MgCl_2$. Senicapoc concentration-response curves of KCNN4 were measured across the range of 0–10 μM senicapoc in the presence of 5 μM A23187 and 100 μM extracellular Ca^{2+}. Senicapoc dilutions were prepared from a frozen stock solution of 1 mM in DMSO.

Cell-attached patch clamp of WT and HX erythrocytes. Cell-attached patch clamp of WT and V282M erythrocytes was performed as previously described (44, 57). Human red cells allowed to settle on coverslips were mounted on an inverted microscope in a 200-μl open chamber (WPI, Sarasota, FL). Symmetric bath and pipette solutions contained (in mM) 140 NaCl, 4 KCl, 1 $CaCl_2$, 1 $MgCl_2$, and 10 HEPES (pH 7.4). Cell-attached patch currents were recorded at room temperature (Axopatch 1-D amplifier, Molecular Devices, Sunnyvale, CA). For current-voltage relationships (I-V curves) in Clampex (PCLAMP10, Molecular Devices), the real-time control window in gap-free mode recorded current traces of 10-to-30 s duration at holding potentials ranging from −100 to +100 mV in 25-mV increments. The bath reference electrode was a silver chloride wire with a 3 M KCl agar bridge. Data were filtered at 500 Hz, digitized at 2 kHz by Clampex, and analyzed offline by Clampfit (PCLAMP10). Holding potentials in on-cell patch experiments were expressed as −Vp, the negative of the pipette potential.

^{45}Ca influx, Ca^{2+} pump activity, and intracellular total Ca^{2+}. Freshly isolated erythrocytes washed three times with normal saline were stored at 4°C as pellets (~80% hematocrit) until use. Calcium fluxes were performed as previously described (40) with modifications. Flux media contained (in mM) 148 NaCl, 2 KCl, 0.15 $MgCl_2$, 10 Tris-MOPS, pH 7.4 at 37°C, 0.1 $CaCl_2$, 10 glucose, and 10 μCi/ml ^{45}Ca. Washed erythrocytes were resuspended at 10% hematocrit in flux media at 37°C. 10 μM A23187 ionophore was added at time zero, followed by immediate vortexing. To test the effect of 1 mM sodium orthovanadate, 50-μl aliquots were transferred from triplicate samples every 15 s into ice-cold Eppendorf tubes containing 1 ml of stop solution (normal saline containing 400 μM $CoCl_2$) overlying 0.3 ml of phthalate oil and centrifuged. After aspiration of supernatants, tube tips containing cell pellets were cut and transferred into scintillation fluid tubes. Pellets were lysed with 300 μl of 0.02% acationox in double-distilled water, followed by the addition of 3 ml of scintillation fluid. Tubes were well mixed and subjected to scintillation counting (Perkin-Elmer). Ca^{2+} pump activity was determined by subtraction of $^{45}Ca^{2+}$ efflux in the presence of 1 mM orthovanadate from that in its absence and expressed as $\mu mol \cdot 10^{13}$ $cells^{-1} \cdot min^{-1}$. Intracellular calcium content at steady state was estimated from $^{45}Ca^{2+}$-loaded cells after 2 h of equilibration at 37°C. One hundred microliter aliquots of ^{45}Ca-loaded cells were centrifuged for 10 s at 4°C through an 800 μl stop solution containing 2 mM Na orthovanadate overlying a 0.4 ml phthalate oil cushion. Cutoff cell pellets were dissolved in 0.02% Acationox and counted. Values corrected by mean cellular volume (MCV) were expressed as picomoles per 10^{13} cells.

Erythrocyte cation and volume modification by nystatin. Nystatin modification of erythrocyte cation content was performed as previously described (11). Freshly isolated erythrocytes washed five times with CWS-Mg were stored at 4°C as pellets (~80% hematocrit). Packed erythrocytes (0.5 ml) were gently resuspended in 5 ml of nystatin loading solution (NLS) containing (in mM) 5–75 NaCl, 75–145 KCl, and 55 or 200 sucrose, respectively, for isotonic or hypertonic conditions. After the addition of nystatin (40 μg/ml) during gentle vortexing, followed immediately by 20-min incubation on ice with mixing at 5-min intervals, cells were centrifuged at 1,500 *g* at 4°C, then resuspended in the same solution lacking nystatin, and again incubated 20 min at 4°C. These nystatin-treated cells were centrifuged and washed four times at 37°C in the same NLS supplemented with 0.5 mM KPO_4, 0.5 mM $NaPO_4$, 10 mM glucose, and 0.1% bovine serum albumin (BSA; fraction V) to remove nystatin. Between each wash, cells were incubated for 10 min at 37°C with gentle shaking. Cells at this stage were again washed five times at 4°C with isotonic CWS-Mg or CWS-Mg rendered hypertonic by the addition of 200 mM sucrose to remove contaminating extracellular Na^+ and K^+. Cell aliquots were then collected for ADVIA analysis of hematological indices, for atomic absorption analysis of intracellular cation content and for $^{86}Rb^+$ influx measurement.

Statistical analysis. Results are expressed as means ± SE. Statistical significance of normally distributed data was determined by one-way ANOVA. Statistical significance of nonparametric data was determined by Mann-Whitney test or Wilcoxon signed-rank test. Differences were judged significant for $P < 0.05$.

RESULTS

Hematological indices of HX V282M erythrocytes. The hematological indices of six individuals of family WO, each affected by HX (5), are presented in Supplemental Table S1 (Supplemental Material for this article is available at https://doi.org/10.6084/m9.figshare.8156198), extending data from two family members presented previously. Affected red cells were macrocytic, hyperchromic, and reduced in number to a degree proportionately greater than the reduction in hemoglobin. The % hyperchromic cells (Hb > 41g/dl) in HX patients was ~36% vs. WT values of <2%. RDW and HDW values in HX patients were also increased. Some indices, such as MCV and reticulocyte count, varied considerably among individual affected family members.

Plasma analyses from the HX V282M patients in this family were remarkable for hyperbilirubinemia, variably elevated LDH, uniformly depressed haptoglobin, and variably elevated ferritin levels in the setting of normal serum iron and transferrin levels (Supplemental Table S2).

Baseline function of HX V282M erythrocytes. Freshly obtained HX V282M erythrocytes were resistant to shear stress-dependent deformation at constant osmolarity, as determined by Rheoscan (Supplemental Fig. S1), as previously observed with erythrocytes analyzed 24–30 h postvenisection by osmotic gradient ektacytometry (44). Reduced deformability was accompanied by elevated intracellular Na content and severely reduced intracellular K content, both of which were exacerbated after 24 h incubation (Supplemental Table S3).

Cell-attached patch recording of WT red cells revealed A23187-stimulated KCNN4 activity completely blocked by senicapoc (SCP; Supplemental Fig. S2*B*). Baseline KCNN4 NPo in unstimulated HX V282M cells was considerably higher than the low values of unstimulated WT cells (Supplemental Fig. S2, *C* and *D*). Elevated baseline HX V282M current was further increased by exposure of cells to Ca^{2+} ionophore A23187 (Supplemental Fig. S2, *A* and *D*), and this incremental current remained sensitive to inhibition by SCP (Supplemental Fig. S2, *A*, *C*, and *D*).

Measurement of stimulated KCNN4-mediated isotopic flux reveals a loss-of-function phenotype for HX mutant V282M red cells. As reported previously (44), baseline SCP-sensitive KCNN4-mediated $^{86}Rb^+$ influx into HX V282M red cells was elevated compared with that of WT cells (Fig. 1*A*). SCP-sensitive flux was intracellular Ca^{2+}-dependent, as it was abrogated by preincubation in BAPTA-AM (Supplemental Fig. S3). Unexpectedly, however, the A23187-stimulated, KCNN4-mediated, SCP-sensitive $^{86}Rb^+$ influx was dramatically reduced in V282M red cells compared with WT cells (Fig. 1*B*). A similar pattern was

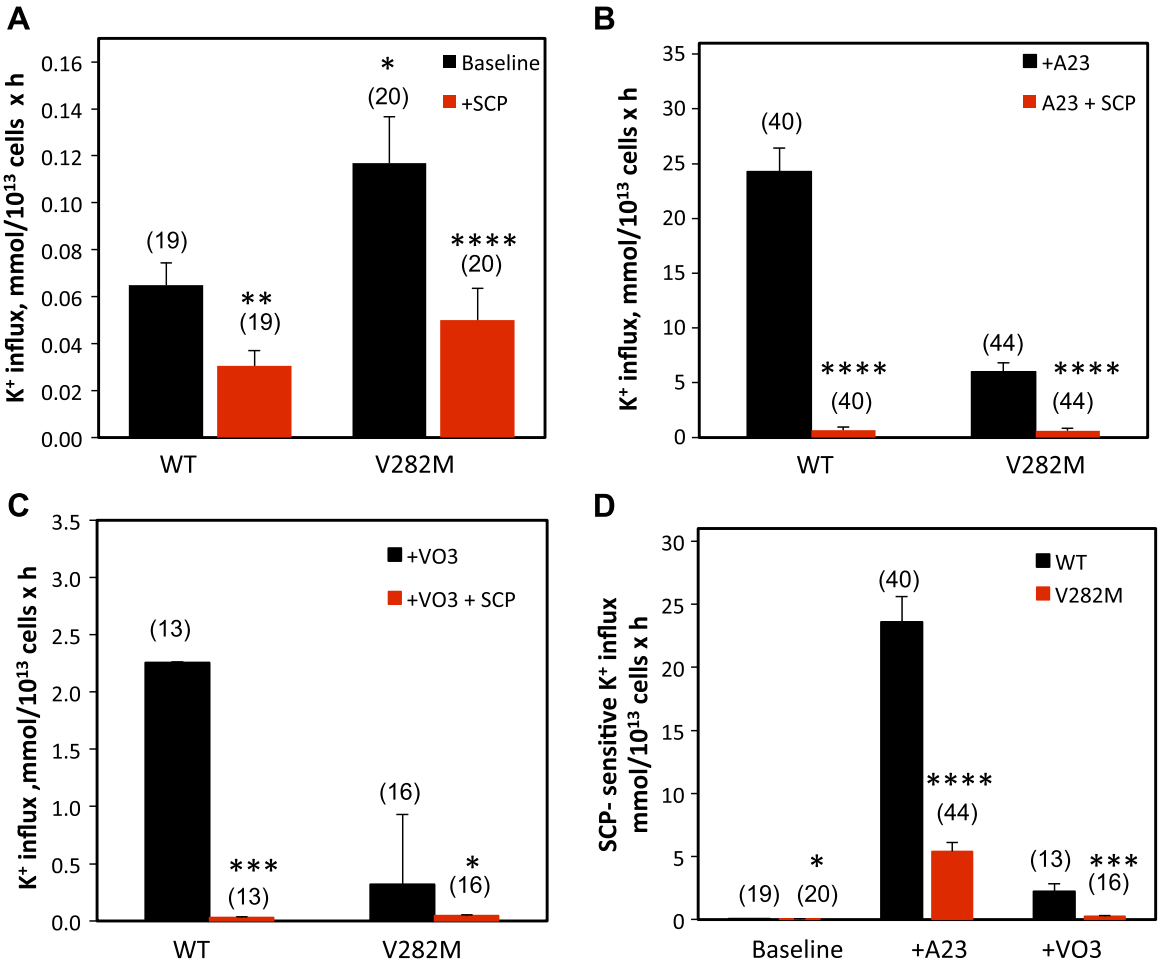

Fig. 1. Activation of KCNN4 by A23187 (A23) or by sodium orthovanadate (VO_3) in wild type (WT) and hereditary xerocytosis (HX; V282M) erythrocytes at 37°C. *A*: freshly isolated erythrocytes incubated in the absence (black) or presence of 200 nM senicapoc (SCP, red) were subjected to measurement of baseline (unstimulated) $^{86}Rb^+$ influx, as described in METHODS. *B*: $^{86}Rb^+$ influx measured in the presence of 5 μM A23187 and 100 μM $CaCl_2$, in the absence and presence of SCP. *C*: $^{86}Rb^+$ influx measured after 30 min preincubation in the presence of 1 mM orthovanadate (VO_3), in the continued presence of VO_3. *D*: SCP-sensitive $^{86}Rb^+$ influx values derived from *A*–*C*. Values in parentheses represent means ± SE for (*n*) experiments, each performed in triplicate, on samples from 5 different HX subjects. $^*P < 0.033$, $^{**}P < 0.0021$, $^{***}P < 0.0002$, and $^{****}P < 0.0001$ comparing absence vs. presence of SCP (Wilcoxon matched pairs test) or comparing V282M vs. WT in the absence of SCP (Mann-Whitney test).

observed comparing HX V282M and WT cells in which intracellular Ca^{2+} was elevated by pretreatment with orthovanadate (Fig. 1*C*). Thus, whereas baseline unstimulated KCNN4 activity in HX V282M red cells exhibited gain-of-function properties in the presence of elevated intracellular [Ca^{2+}] produced by A23187-mediated enhanced extracellular Ca^{2+} entry or by orthovanadate-mediated blockade of PMCA Ca^{2+}-ATPase-mediated Ca^{2+} efflux, KCNN4 V282M activity exhibited a previously undescribed loss-of-function phenotype (Fig. 1*D*). The senicapoc-sensitive relative increase in % hyperchromic cells (Fig. 2, *A* and *C*), and to a lesser extent in CHCM (Fig. 2*B*,D), was also reduced in HX V282M cells compared with WT cells after treatment with orthovanadate or with A23187 exposure (Fig. 2, *A* and *C*).

Ca^{2+} and senicapoc sensitivity of HX V282 red cells. This surprising loss-of-function phenotype prompted evaluation in WT and V282M red cells of concentration-response relationships for senicapoc and for [Ca^{2+}]. As previously reported for recombinant KCNN4 V282M in HEK-293 cells (42) and for unstimulated KCNN4 activity in HX V282M red cells (44), KCNN4 activity in WT red cells and KCNN4 activity in HX red cells expressing heterozygous KCNN4 V282M exhibited similar senicapoc ID_{50} values of 1.94 ±0.5 and 0.69 ± 0.2 nM, respectively (Fig. 3, *A* and *B*). However, these ID_{50} values were approximately five to 10-fold lower than reported for whole cell currents in HEK-293 cells (42). Native erythroid KCNN4 Ca^{2+} sensitivity measured by A23187 equilibration of intracellular [Ca^{2+}] with varying extracellular [Ca^{2+}] allowed estimates of [Ca^{2+}] EC_{50} values for KCNN4 of 1.02 ± 0.1 μM in WT erythrocytes and 1.20 ± 0.01 μM in HX V282M erythrocytes (Fig. 3*C*). As noted previously (44), both EC_{50} values exceed those measured by whole cell patch clamp of HEK-293 cells (42). Thus, although native WT and heterozygous KCNN4 V282M activities measured by $^{86}Rb^+$ influx in red cells differed slightly from those measured by whole cell patch clamp in HEK-293 cells, the apparent "loss-of-function" phenotype of HX V282M red cells does not reflect altered intracellular Ca^{2+} affinity or senicapoc sensitivity of KCNN4 as measured in those red cells.

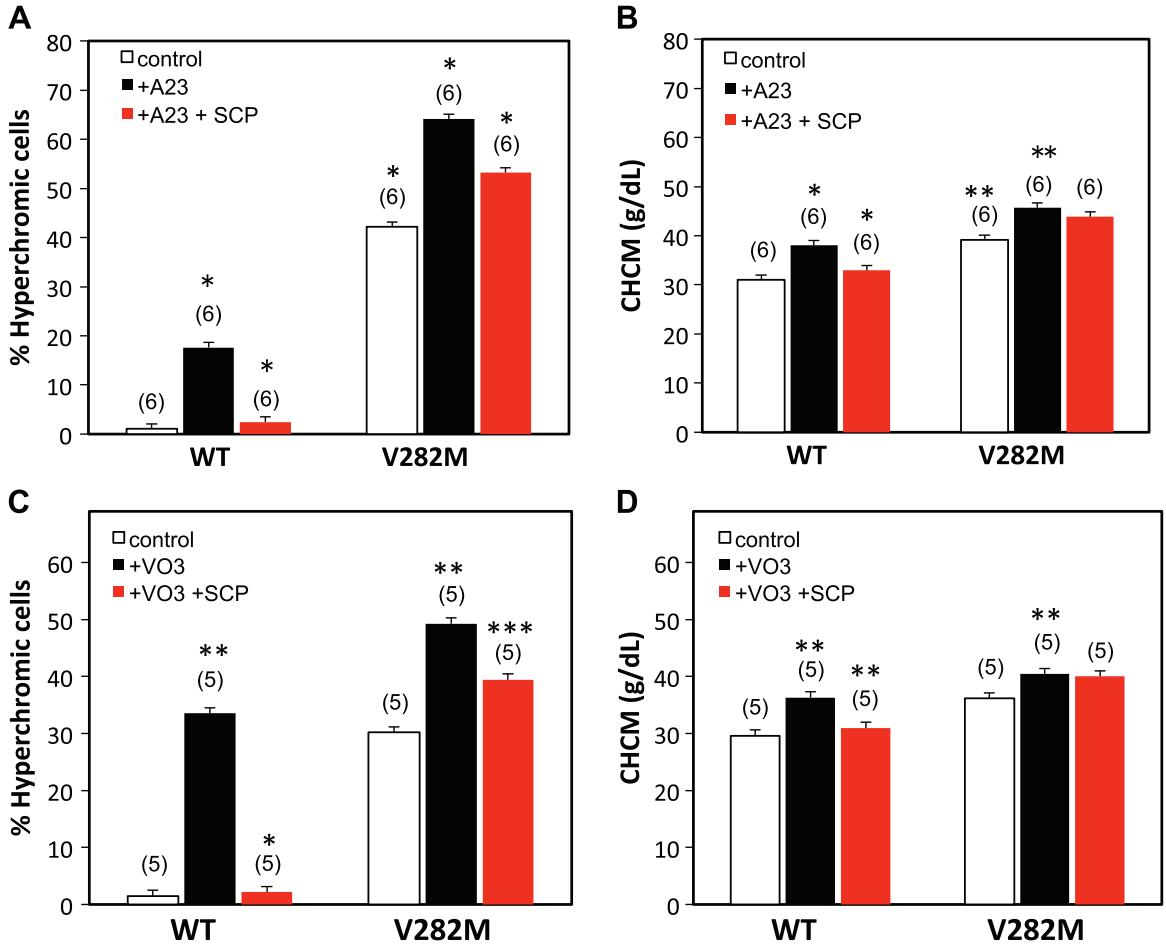

Fig. 2. Senicapoc (SCP) inhibition of wild type (WT) red blood cell (RBC) dehydration induced by A23187 (A23) or by orthovanadate (VO_3) at 37°C is attenuated in V282M hereditary xerocytosis (HX) RBC. *A* and *B*: freshly isolated cells were incubated for 10 min at 37°C in the absence (white) or presence (black and red) of 5 μM A23 and 100 μM $CaCl_2$, in the absence or presence of 200 nM SCP, followed by hematological analysis (ADVIA). Values represent means ± SE from (*n*) experiments. *$P < 0.033$; **$P < 0.01$ (Wilcoxon signed-rank test), comparing the absence of A23 or SCP; ***$P < 0.001$ (Mann-Whitney test), comparing WT vs. HX V282M. *C* and *D*: freshly isolated cells were incubated with or without 1 mM orthovanadate (VO_3) in the presence of 1.5 mM $CaCl_2$ for 1 h at 37°C in the presence (red) or absence of 200 nM SCP (white and black), after which cells were subjected to hematological analysis (ADVIA). Values represent means ± SE for (*n*) experiments performed on samples from 4 different HX subjects. *$P = 0.02$, **$P = 0.002$ (Wilcoxon signed-rank test).

Ca^{2+} transport activity in HX V282M red cells. The reduced activity of stimulated KCNN4 in HX V282M red cells might reflect altered Ca^{2+} handling. However, A23187-induced $^{45}Ca^{2+}$ entry into HX V282M red cells in the presence of orthovanadate blockade of Ca^{2+} efflux was equivalent to or slightly greater than that into WT cells (Fig. 4*A*). Although the rapid phase of Ca^{2+} entry was slightly delayed in HX cells, early plateau $^{45}Ca^{2+}$ accumulation was at least equivalent to that of WT cells (Fig. 4*B*) and at later times exceeded that of WT cells (Fig. 4*C*). Consistent with these results, vanadate-sensitive Ca^{2+} efflux rates (reflecting PMCA activity) were lower in HX V282M than in WT red cells (Fig. 4, *D–F*). Thus, these results did not explain a loss-of-function KCNN4 phenotype in HX V282M red cells.

Calpain inhibitor response in HX V282M red cells. Calpain-1-knockout mouse erythrocytes exhibited decreased A23187-stimulated KCNN4 activity (58). Chronic in vivo treatment with calpain inhibitor BDA-410 also reduced KCNN4 activity and hypoxia-induced red cell dehydration in the SAD mouse model of sickle cell disease and altered KCNN activity in red cells from WT mice (19). Although interpreted as KCNN4 regulation by PKC or peroxiredoxin, the results may have reflected inhibition of calpain-mediated KCNN4 cleavage. We found, however, that calpain inhibitor PD150606 substantially stimulated baseline KCNN4 activity in WT human red cells and stimulated baseline KCNN4 activity in HX V282M cells to a lower degree (Fig. 5*A*). A23187-stimulated KCNN4 activity was further increased by PD150606, whereas the much lower KCNN4 activity measured in A23187-stimulated HX V282M cells was not increased further by the calpain inhibitor (Fig. 5*B*). Assuming specificity of the calpain inhibitor's effects used at high concentration, these results suggest that proportional calpain sensitivity of KCNN4 or its regulators is maintained in unstimulated HX V282M cells, but to a reduced extent in stimulated HX V282M cells. The observed stimulation of human erythroid KCNN4 by a calpain inhibitor is, to our knowledge, novel.

Stimulated KCNN4 activity of WT red cells can be converted to the reduced activity phenotype of HX V282M cells by hypertonic shrinkage and modulation of intracellular monovalent cation content. We hypothesized that the altered cation contents of HX V282M red cells might contribute directly to the reduced sensitivity of KCNN4 in HX V282M red cells to

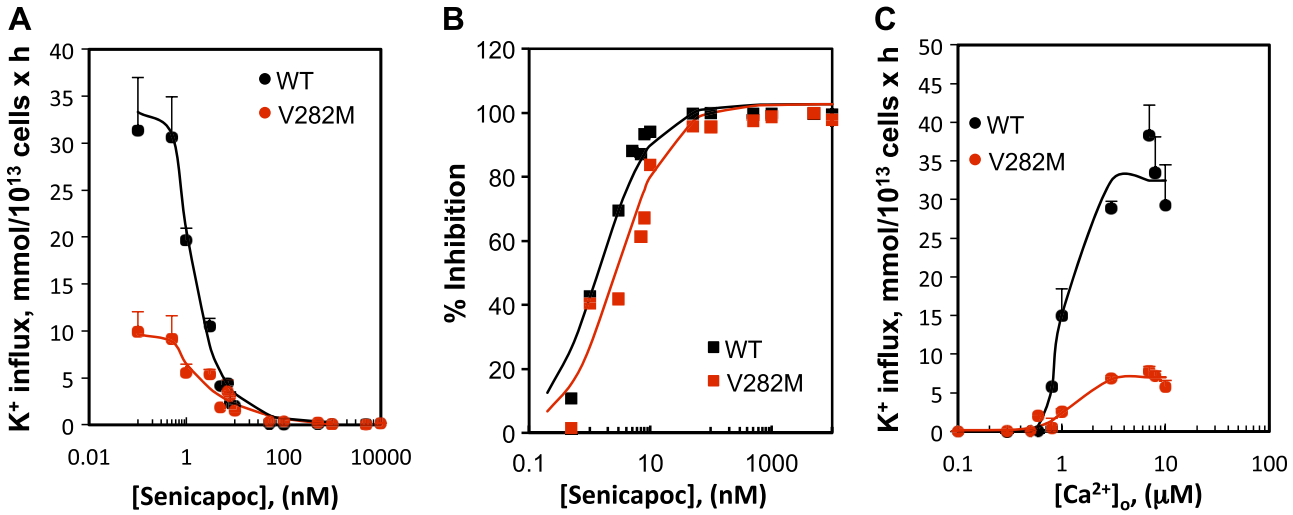

Fig. 3. Senicapoc concentration-response relationships and extracellular Ca^{2+} (Ca^{2+}_o) activation curves of KCNN4 in intact A23187-stimulated wild type (WT) and V282M hereditary xerocytosis (HX) erythrocytes. *A*: $^{86}Rb^+$ influx was measured at room temperature in freshly isolated erythrocytes stimulated with A23187 in the presence of senicapoc concentrations ranging from 0 to 10 μM ($n = 4$). Calculated IC_{50} for senicapoc was 1.94 ± 0.5 nM for WT and 0.69 ± 0.2 nM for V282M. KCNN4 activity was measured as in METHODS. *B*: data in *A* plotted as relative % inhibition of KCNN4 activity. *C*: Ca^{2+} activation of $^{86}Rb^+$ influx was measured at the indicated nominal intracellular Ca concentrations equilibrated with extracellular bath in EGTA or citrate buffer in the presence of A23187, as previously described (43). EC_{50} values for nominally equilibrated Ca^{2+}_o were 1.02 μM for WT and 1.20 μM for V282M. Data are means ± SE ($n = 5$), each performed in triplicate on samples from 3 different HX subjects.

activation by A23187 or vanadate, rather than merely reflect the increased cation leak of HX cells. Previous studies have demonstrated inhibition of KCNN4 activity by Na^+ loading and K^+ depletion in resealed red cell ghosts (59) and in intact red cells subjected to overnight pretreatment in cation-permeabilizing cold thiocyanate medium (54). In this context, we tested whether nystatin modification of WT red cell cation content to resemble that of HX red blood cells (RBC) might elicit reduction in the stimulated KCNN4 response corresponding to the suppressed KCNN4 stimulation of HX V282M cells. Incubation of wild-type red cells in nystatin load solution (40Na:110K) containing 200 mM sucrose elevated intracellular Na content to baseline HX V282M levels and reduced intracellular K content to below baseline HX V282M levels (Table 1) while increasing WT values of MCHC, CHCM, and % hyperchromic cells approximately to baseline HX V282M values (Tables 2 and 3). The resulting modified WT cells were more microcytic than HX red cells. A23187-stimulated KCNN4 activity in WT cells was reduced by nystatin treatment in these conditions, but not to the low level of A23187-stimulated activity in nystatin-untreated HX V282M cells (Fig. 6*A*). However, orthovanadate-stimulated KCNN4 activity in nystatin-treated WT red cells was suppressed to or below the KCNN4 activity of vanadate-stimulated, nystatin-untreated HX V282M cells (Fig. 6*B*).

Thus, nystatin manipulation of intracellular Na and K contents in the setting of hypertonic shrinkage partially converted the WT KCNN4 response to A23187 and completely converted the WT KCNN4 response to orthovanadate to resemble the corresponding responses of nystatin-untreated HX V282M red cells. Alternately stated, the orthovanadate-stimulated KCNN4 phenotype of WT cells was converted to that of HX V282M cells by combined hypertonic shrinkage and nystatin-induced elevation of cell Na and reduction of cell K. The A23187-stimulated KCNN4 phenotype of WT cells was only partially converted to that of HX V282M cells by nystatin treatment in these conditions.

Can the phenotype of abnormally low stimulated KCNN4 activity of HX V282M red cells be converted to that of WT red cells by normalizing intracellular monovalent cation content? We showed above that the stimulated KCNN4 phenotype of WT red cells can be converted to that of HX V282M cells. We next considered the clinically more interesting possibility of converting the stimulated KCNN4 activity phenotype of HX V282M cells to that of WT cells. We compared KCNN4 activity of untreated WT and HX V282M red cells at baseline and after nominally isotonic nystatin treatment either to mimic normal intracellular cation concentrations (10Na:135K) or to mimic intracellular cation concentrations of HX (75Na:75K) (Table 1). KCNN4 baseline activity in nystatin-untreated HX red cells was higher than in WT cells (Fig. 7*A*), but orthovanadate-stimulated KCNN4 activity was much higher in WT than in HX cells (Fig. 7*D*).

Baseline KCNN4 activity patterns were preserved in both cell types after nystatin treatment at 10Na:135K to mimic normal intracellular cation concentrations, although WT baseline activity was relatively higher than in nystatin-untreated cells (Fig. 7*B*). Nystatin 10:135 preincubation of HX V282M cells reduced and normalized intracellular Na but only moderately elevated intracellular K (Table 1). These nystatin conditions also normalized the elevated MCHC, CHCM, and % hyperchromic cells of HX V282M at the cost of cell enlargement beyond the baseline macrocytosis of these HX V282M cells (Tables 2 and 3).

Thus, partial normalization of ion content in HX red cells did not alter the baseline gain-of-function phenotype of KCNN4 V282M in HX red cells. However, the combination of nystatin 10Na:135K pretreatment with orthovanadate stimulation reduced orthovanadate-stimulated KCNN4 activity by 90–95% in WT red cells and by 50–70% in orthovanadate-

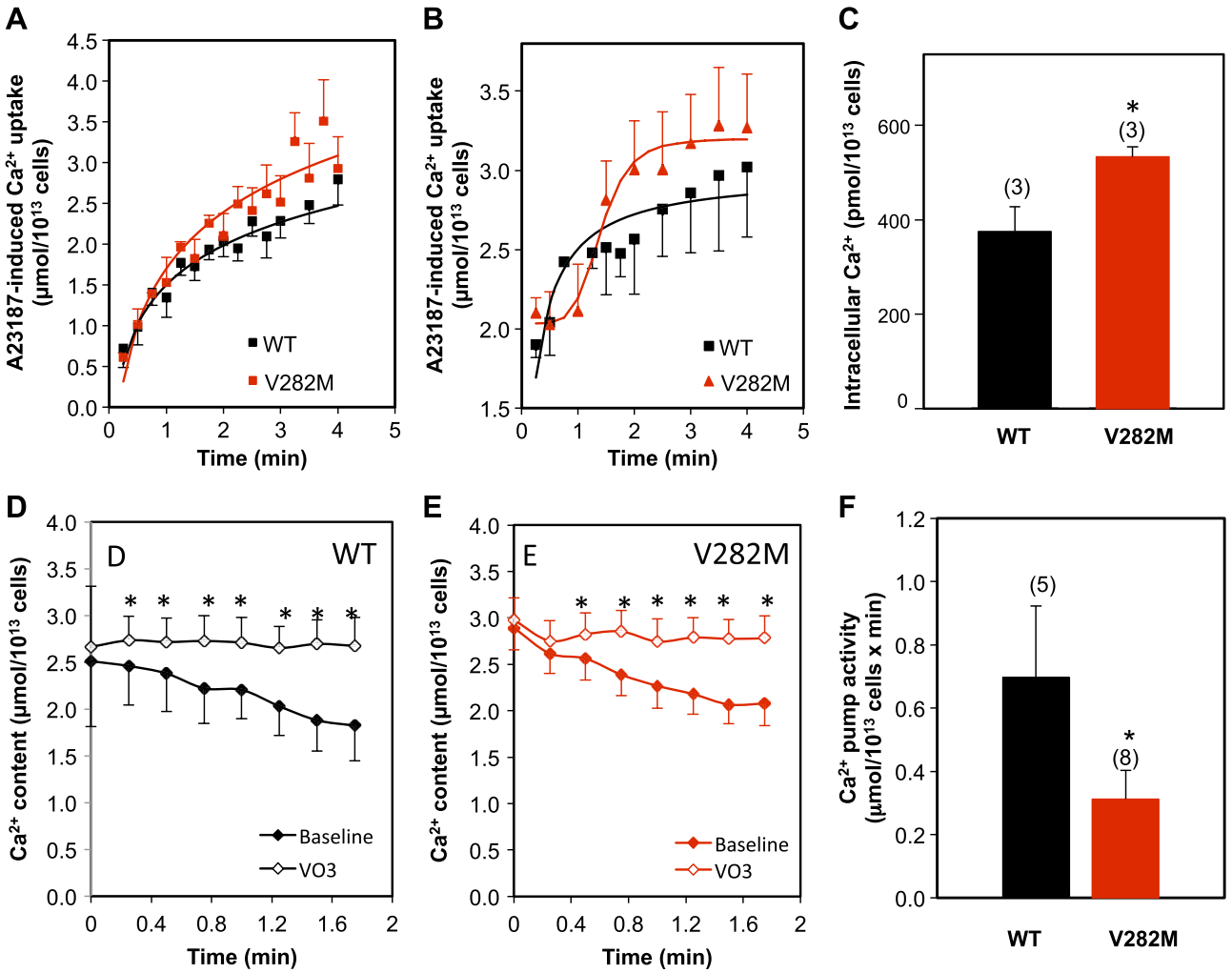

Fig. 4. A23187-stimulated Ca^{2+} uptake and plasmalemmal Ca^{2+}-ATPase (PMCA)-mediated Ca^{2+} efflux in wild type (WT) and V282M hereditary xerocytosis (HX) erythrocytes. *A*: time-dependent 5 µM A23187-induced Ca^{2+} uptake at 37°C in WT (black) and V282M HX erythrocytes (red) in normal saline containing 100 µM $CaCl_2$ and 10^{-8} M ^{45}Ca (means ± SE; $n = 4$ triplicate experiments). *B*: time-dependent 5 µM A23187-induced Ca^{2+} uptake at 37°C in WT (black; $n = 4$) and V282M HX erythrocytes (red; $n = 3$), initiated following 30 min preincubation in 1 mM orthovanadate (VO_3) with continued presence of orthovanadate (means ± SE, with each experiment performed in triplicate). *C*: steady-state (2 h) Ca^{2+} uptake at 37°C into WT (black) and V282M erythrocytes (red, 10% hematocrit) in the presence of 1.8 mM bath $CaCl_2$ (10^{-7} M $^{45}Ca^{2+}$) and 1 mM orthovanadate (without A23187). Means ± SE of 3 experiments performed in triplicate. *$P < 0.041$ (Mann-Whitney test). *D* and *E*: time-dependent Ca^{2+} efflux from WT (black; *D*) or HX V282M red blood cells (RBC) (red; *E*) after 30 min preincubation in the absence (closed diamonds) or presence of 1 mM orthovanadate with continued presence of orthovanadate (open diamonds). Means ± SE ($n = 3$), each performed in triplicate; *$P < 0.0001$ (paired *F*-test). *F*: PMCA activity calculated from efflux activity data in *D* and *E* (means ± SE of 5 or 8 experiments, each performed in triplicate at 37°C). Data represent determinations on samples from 3 different HX subjects. *$P < 0.01$ (Mann-Whitney test).

stimulated KCNN4 activity in HX V282M cells without abrogating orthovanadate stimulation (Fig. 7, *D* vs. *E*). Moreover, orthovanadate-stimulated KCNN4 activity in WT and HX V282M cells treated with nystatin at 10Na:135K differed only minimally, such that the KCNN4 mutant V282M gain-of-function phenotype with respect to WT KCNN4 was not apparent. Thus, nystatin treatment at 10Na:135K normalized the proportional relationship between vanadate-stimulated KCNN4 activity of HX V282M red cells with that of WT red cells. However, this "rescue" was complicated by the accompanying severe reduction in stimulated activity in both cell types.

After nystatin pretreatment in 75Na:75K conditions, baseline KCNN4 activity in WT red cells was higher (Fig. 7*C*) than in nystatin-untreated WT cells (Fig. 7*A*), whereas baseline KCNN4 activity in HX V282M red cells was much lower (Fig. 7*C*) than in nystatin-untreated HX cells (Fig. 7*A*). Nystatin treatment at 75Na:75K reduced vanadate-stimulated KCNN4 activity ~90% in both WT and HX V282M cells (Fig. 7*F*) from levels in nystatin-untreated cells (Fig. 7*D*). However, even with these greatly reduced activities, orthovanadate-stimulated KCNN4 activity in HX V282M cells was only 20% that of WT cells (Fig. 7*F*).

The increased % hyperchromic cells of HX V282M genotype in either the absence or presence of orthovanadate stimulation (Fig. 8*A*) was nearly normalized upon nystatin-mediated normalization of intracellular cation content (Fig. 8*B* and Table 1). However, nystatin treatment at 75Na:75K restored baseline % hyperchromic cells but abrogated the effect of orthovanadate on hyperchromic cell number (Fig. 8*C*). Partial

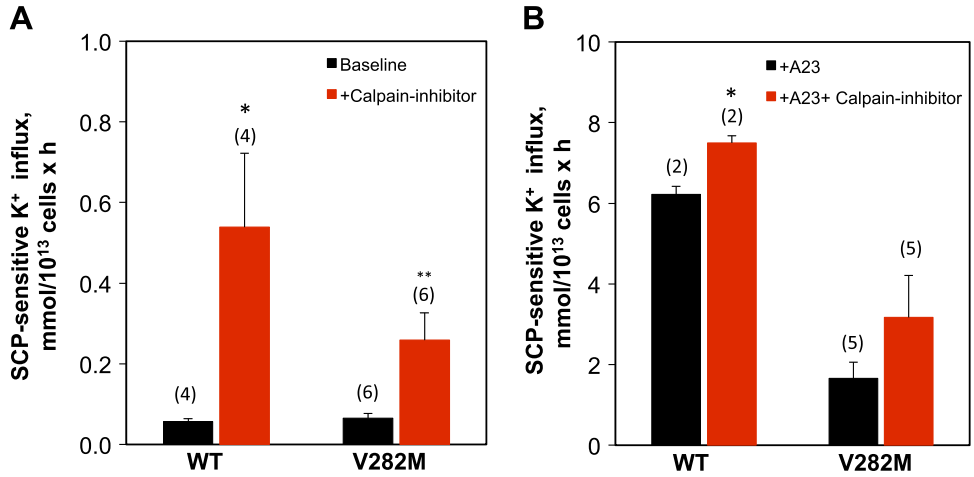

Fig. 5. Effect of cell-permeant calpain inhibitor PD150606 on senicapoc (SCP)-sensitive $^{86}Rb^+$ influx in wild type (WT) and V282M erythrocytes. Baseline (*A*) or A23187-stimulated, SCP-sensitive $^{86}Rb^+$ influxes (*B*) were measured in freshly isolated erythrocytes preincubated at 10% hematocrit for 45 min at 37°C in the absence or presence of 500 μM PD150606 in normal saline containing 10 mM glucose and 1.5 mM $CaCl_2$. Cells were centrifuged and resuspended in 37°C flux media, and baseline or A23187 (A23)-stimulated fluxes were measured in the continued absence or presence of 500 μM PD150606 with or without 200 nM senicapoc (SCP). The senicapoc-sensitive component of flux here (and in all subsequent figures) was calculated as in Fig. 1. Data are means ± SE for (*n*) experiments, each performed in triplicate, on samples from 3 different hereditary xerocytosis (HX) and 2 WT subjects. $*P < 0.028$, $**P = 0.002$ comparing presence and absence of calpain inhibitor (Mann-Whitney test).

normalization of HX V282M cell cation content largely preserved orthovanadate responsiveness of MCV (Fig. 8, *D* and *E*) and MCHC (Fig. 8, *G* and *H*). Nystatin treatment of HX V282M cells at 75Na:75K abrogated orthovanadate-induced changes in MCV (Fig. 8, *D* and *F*) and MCHC (Fig. 8, *G* and *I*).

Intracellular monovalent cation concentration dependence of the maximally stimulated KCNN4 activity phenotype. We next sought to determine thresholds for nystatin-induced changes in intracellular cation contents of WT and V282M red cells that might interconvert the orthovanadate-stimulated KCNN4 phenotypes of the two cell genotypes. Baseline KCNN4 activity was invariant across the range of tested intracellular cation contents in WT red cells (Fig. 9*A*). The higher baseline KCNN4 activity of HX V282M red cells was also statistically unchanged across the range of cation concentrations, but high variance in measurements may have obscured a decrease upon lowering K content and elevating Na content (Fig. 9*D*). In contrast, A23187-stimulated KCNN4 activity in nystatin-treated WT red cells was most active at lower intracellular Na and higher intracellular K, and fell with further Na elevation and K reduction (Fig. 9*B*). The lower A23187-stimulated KCNN4 activity of HX V282M red cells exhibited a qualitatively similar pattern of dependence on altered intracellular cation content (Fig. 9*E*). Even the greatly reduced levels of orthovanadate-stimulated KCNN4 activity observed in nystatin-pretreated red cells of both genotypes were further inhibited in graded fashion by elevation of intracellular Na and reduction of intracellular K contents. The intracellular cation content dependence of orthovanadate-stimulated KCNN4 activity in nystatin-treated WT red cells at intracellular Na:K ratios of 8:256 or 28:224 (mmol/kg Hb) had no effect, but KCNN4 activity was severely suppressed at Na:K ratios of 60:136 or 90:98 (Fig. 9*C*). The yet lower levels of orthovanadate-stimulated KCNN4 activity in nystatin-treated HX V282M cells were also further suppressed by elevated intracellular Na and reduced intracellular K contents (Fig. 9*F*).

Table 1. *Cation content of nystatin-treated wild type and V282M HX erythrocytes*

ID	*n*	$[Na]_i$, mmol/Kg Hb	$[K]_i$, mmol/kg Hb	[Sucrose], mM
WT				
Baseline	18	24.3 ± 0.9	295.2 ± 11	0
NyLS 10:135	4	21.49 ± 0.3	231.27 ± 12	55
NyLS 75:75	4	68.1 ± 2	86.1 ± 5	55
NyLS 40:110	3	39.8 ± 0.6	95.0 ± 0.7	200
V282M				
Baseline	18	37.3 ± 2**	164.7 ± 7**	0
NyLS 10:135	7	21.44 ± 3	176.2 ± 11*	55
NyLS 75:75	6	74.4 ± 4	93.7 ± 8	55

Freshly isolated wild type (WT) and V282M HX erythrocytes pretreated without (baseline) or with nystatin in nystatin loading solutions (NyLS) containing the indicated concentrations of Na and K (in mM:mM, leftmost column) and of sucrose (rightmost column) were suspended in CWS-Mg as described in METHODS. Ion content was measured by atomic absorption spectroscopy. Values represent means ± SEM of (*n*) experiments, each performed in triplicate on samples from 5 different HX subjects. $*P < 0.033$; $**P < 0.0021$ for WT vs. V282M (Mann-Whitney test).

These data demonstrate that nystatin treatment in physiological saline yielding a near physiological intracellular cation ratio of 8 Na: 256 K (mmol/kg Hb) preserves the loss-of-function phenotype of A23187- or orthovanadate-stimulated KCNN4 activity in HX V282M red cells as compared with WT cells. However nystatin-treated WT and HX V282M cells in which intracellular Na and K contents were equalized exhibited comparably severe reductions in KCNN4 activity in both WT and HX V282M red cells (Fig. 9, *B–F*).

Is the phenotype of reduced maximal stimulation of KCNN4 activity unique to HX red cells of patients heterozygous for KCNN4 V282M? The loss-of-function phenotype for V282M red cell KCNN4 activity stimulated by A23187 or by vanadate in HX V282M red cells contrasts markedly with the gain-of-function phenotype for baseline KCNN4 activity in the same cells. However, stimulated KCNN4 activity in HX red cells of

Table 2. *Hematological indices of wild type erythrocytes and wild type erythrocytes treated with nystatin*

	WT (n = 3)	WT-Ny (40:110) (n = 3)	WT-Ny (10:135) (n = 6)*	WT-Ny (75:75) (n = 4)
MCHC, g/dl	33.5 ± 1.2	38.2 ± 0.9	28.4 ± 2	28.9 ± 0.8
CHCM, g/dl	34.4 ± 0.4	41.0 ± 0.3	31.3 ± 0.7	33.2 ± 0.8
% Micro	0.87 ± 0.5	3.0 ± 1.2	0.35 ± 0.1	0.9 ± 0.3
% Hyper	3.8 ± 1.2	43.1 ± 6.5†	3.4 ± 2	2.85 ± 0.2
RDW, %	14.3 ± 0.6	13.7 ± 0.8	14.4 ± 0.7	14.7 ± 0.3
MCV, fl	91.6 ± 2.9	83.5 ± 1.8	99.0 ± 4	89.5 ± 0.5
Retics, %	2.8 ± 0.6	2.3 ± 1	1.8 ± 0.8 (3)	1.72 ± 0.3

ADVIA hematological indices of WT erythrocytes untreated and pretreated with nystatin (WT-Ny) in the presence of solutions containing (in mM:mM) Na and K at 40:110, 10:135, and 75:75. Values are means ± SEM for (n) experiments on samples from 5 different HX subjects, with (n)* denoting a smaller (n = 3) for retics. †$P < 0.025$ vs. WT (paired Wilcoxon signed-rank test).

other mutant genotypes has been reported to date only in association with KCNN4 mutation R352H (41, 42) or with several PIEZO1 mutations (14, 33, 42). Therefore, we compared baseline and stimulated KCNN4-mediated $^{86}Rb^+$ influx activities in red cells from HX patients with several additional types of mutations, whose hematological indices are assembled in Supplemental Table S4.

As shown in Supplemental Fig. S4*A*, orthovanadate-stimulated KCNN4 activity was elevated in HX red cells from a single patient heterozygous for KCNN4 mutation R352H (5) as compared with WT red cells. However, this gain-of-function phenotype in HX versus WT cells was not evident when assayed as A23187-stimulated KCNN4 activity (Supplemental Fig. S5*A*).

HX RBC from three additional HX patients with PIEZO1 mutations were also examined. Whereas baseline KCNN4 activity in HX RBC from patients heterozygous for PIEZO1 mutations R2488Q (7) and V598M (23) was higher than in WT red cells, orthovanadate-stimulated KCNN4 activity in both types of PIEZO1 mutant HX red cells was substantially lower than that of WT red cells (Supplemental Fig. S4, *B* and *C*). In contrast, the baseline KCNN4 activity gain-of-function phenotype of HX red cells from a patient heterozygous for PIEZO1 R2456H (49) was maintained as a gain-of-function phenotype in the presence of vanadate (Supplemental Fig. S4*D*). Thus, as evaluated through orthovanadate-stimulated, senicapoc-sensitive $^{86}Rb^+$ influx, HX red cells expressing KCNN4 or PIEZO1 mutant polypeptides can exhibit either gain-of-function or loss-of-function phenotypes.

Table 3. *Hematological indices of nystatin-untreated and nystatin-treated HX V282M erythrocytes*

	V282M (n = 3)	V282M-Ny (10:135) (n = 8)*	V282M-Ny (75:75) (n = 6)*
MCHC, g/dl	39.1 ± 0.6	31.2 ± 0.5‡	33.5 ± 0.6
CHCM, g/dl	41.2 ± 0.7	33.8 ± 1†	39.1 ± 0.3‡
%Micro	0.4 ± 0.1	0.15 ± 0.1	0.42 ± 0.1
%Hyper	52.6 ± 7	4.8 ± 1†	26.1 ± 3†
RDW, %	14.7 ± 0.6	15.6 ± 0.4	15.2 ± 0.3
MCV, fl	96.9 ± 1.6	107.0 ± 1.5†	98.9 ± 2.3
Retics, %	10.8 ± 0.9	0.94 ± 0.6 (4)§	7.26 ± 0.8 (5)

ADVIA hematological indices of HX V282M erythrocytes untreated (V282M) or pretreated with nystatin (V282M-Ny) in the presence of solutions containing (in mM:mM) Na and K at 10:135 or 75:75. Values are means ± SEM for (n) experiments on samples from 3 different HX subjects, with (n)* denoting a smaller (n) for % retics. †$P < 0.025$; ‡$P < 0.04$; §$P < 0.002$ compared with V282M (paired Wilcoxon signed-rank test).

Characterization of individual HX mutations as gain or loss of function was further complicated by evaluation of A23187-stimulated, senicapoc-sensitive $^{86}Rb^+$ influx (Supplemental Fig. S5). HX red cells from the patient carrying PIEZO1 mutation R2456H maintained gain of stimulated function in the presence of A23187 compared with WT cells (Supplemental Fig. S5*D*). In contrast, PIEZO1 R2488Q HX red cells exhibited A23187-stimulated KCNN4 activity only marginally lower than WT cells (Supplemental Fig. S5*B*), and HX red cells carrying the robust KCNN4 gain-of-orthovanadate-stimulated-function mutation R352H show A23187-stimulated function at WT levels (Supplemental Fig. S5*A*). Moreover, HX red cells carrying the robust PIEZO1 loss-of-orthovanadate-stimulated function mutation V598M also exhibit A23187-stimulated function equivalent to that of WT red cells (Supplemental Fig. S5*C*).

Thus, in HX red cells of all genotypes tested to date, unstimulated KCNN4 activity was higher than unstimulated levels in WT red cells. However, stimulated KCNN4 activity in HX red cells, measured as orthovanadate-stimulated or A23187-stimulated $^{86}Rb^+$ influx, was either lower than, higher than, or equivalent to WT activity. These patterns were mutation specific whether HX reflected mutations in KCNN4 or PIEZO1.

DISCUSSION

Autosomal dominant or spontaneous hereditary xerocytosis (HX) is a hemolytic anemia attributed to gain-of-function mutations in the PIEZO1 or KCNN4 polypeptides of the red cell membrane, all leading to increased red cell K^+ loss and dehydration. The mechanisms by which red cell dehydration leads to decreased red cell deformability, sequestration, hemolysis, and shortened erythrocyte lifespan in the circulation remain incompletely understood. Our present study has investigated the unexpected dual gain- and loss-of-function phenotypes of the HX KCNN4 mutant V282M as expressed in red cells assayed by measurement of isotopic fluxes. Baseline senicapoc-sensitive KCNN4 activity of HX V282M red cells was higher than in WT red cells whether measured as $^{86}Rb^+$ influx (Fig. 1, *A* and *D*) or by cell-attached patch clamp (Supplemental Fig. S3 and Ref. 44). In contrast, senicapoc-sensitive KCNN4-mediated $^{86}Rb^+$ influx stimulated by A23187 or by orthovanadate was much lower in HX V282M red cells than in WT cells (Fig. 1, *B–D*). Secondary reduction in a possible rate-limiting chloride conductance in HX V282M red cells was considered unlikely, as suppression of stimulated KCNN4 activity in these cells was neither rescued nor attenuated

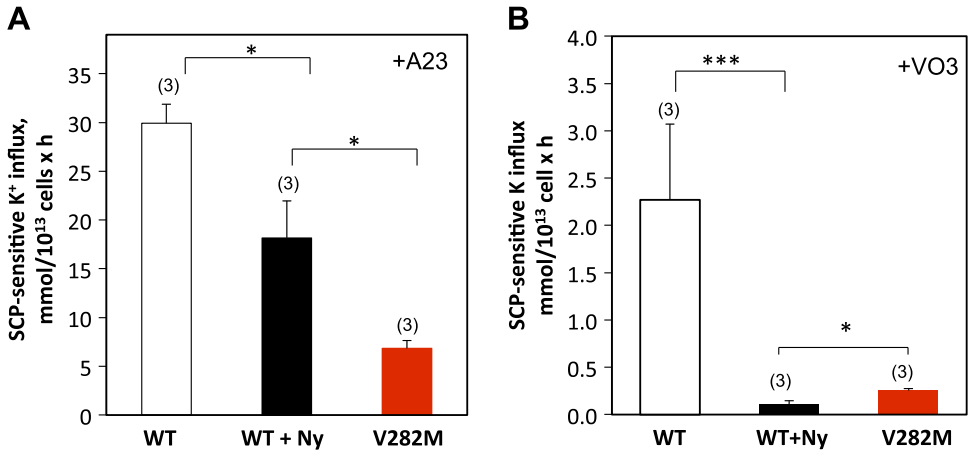

Fig. 6. Combined nystatin treatment and dehydration of wild type (WT) erythrocytes decreases stimulated KCNN4 activity induced by A23187 (A23) or by orthovanadate (VO_3). 200 nM senicapoc (SCP)-sensitive $^{86}Rb^+$ influx stimulated by 5 μM A23 (A23, *A*) or by 1 mM orthovanadate (VO_3, *B*) was measured at 37°C in wild-type (WT) erythrocytes treated without (white bars) or with nystatin (Ny; black bars) in chloride solution containing (in mM:mM) 40 Na:110 K + 200 mM sucrose) and compared with those values in nystatin-untreated V282M cells (red bars). Values represent means ± SE ($n = 3$), each performed in triplicate, on samples from 2 different hereditary xerocytosis (HX) subjects. *$P < 0.028$ in *A*. ***$P < 0.0002$ and *$P < 0.028$ in *B* (Mann-Whitney tests).

by flux medium replacement of 10 mM Cl^- with equimolar thiocyanate, a more highly permeant anion (not shown).

Insights from KCNN4 structure. The baseline gain-of-function phenotype of KCNN4 mutant V282M may reflect closed-state destabilization due to steric clash of the Met side chains with intermittent widening of the WT channel's closed-state inner pore radius of <1 Å (28), possibly facilitating partial population of KCNN4 activated state I (or even state II) at resting red cell [Ca^{2+}]. Conversely, the maximally activated loss-of-function phenotypes in the presence of A23187 or orthovanadate may reflect reduction of WT inner pore diameter in KCNN4 activated states I and/or II by the Met282 side chain, resulting in decreased maximal ion transport, with or without changes in activated state occupancies (28). As heterozygous V282M red cells express a mix of WT and V282M homotetramers and of V282/M282 heterotetramers in (ideally) a binomial distribution of KCNN4 protomer stoichiometries, assessment of coexpression and concatamer expression could characterize stoichiometry-dependent functional differences among tetrameric subtypes.

Genotype specificity of the HX loss-of-function phenotype. Combined gain- and loss-of-function phenotypes are not limited to KCNN4 HX mutant red cells. Indeed, a recent

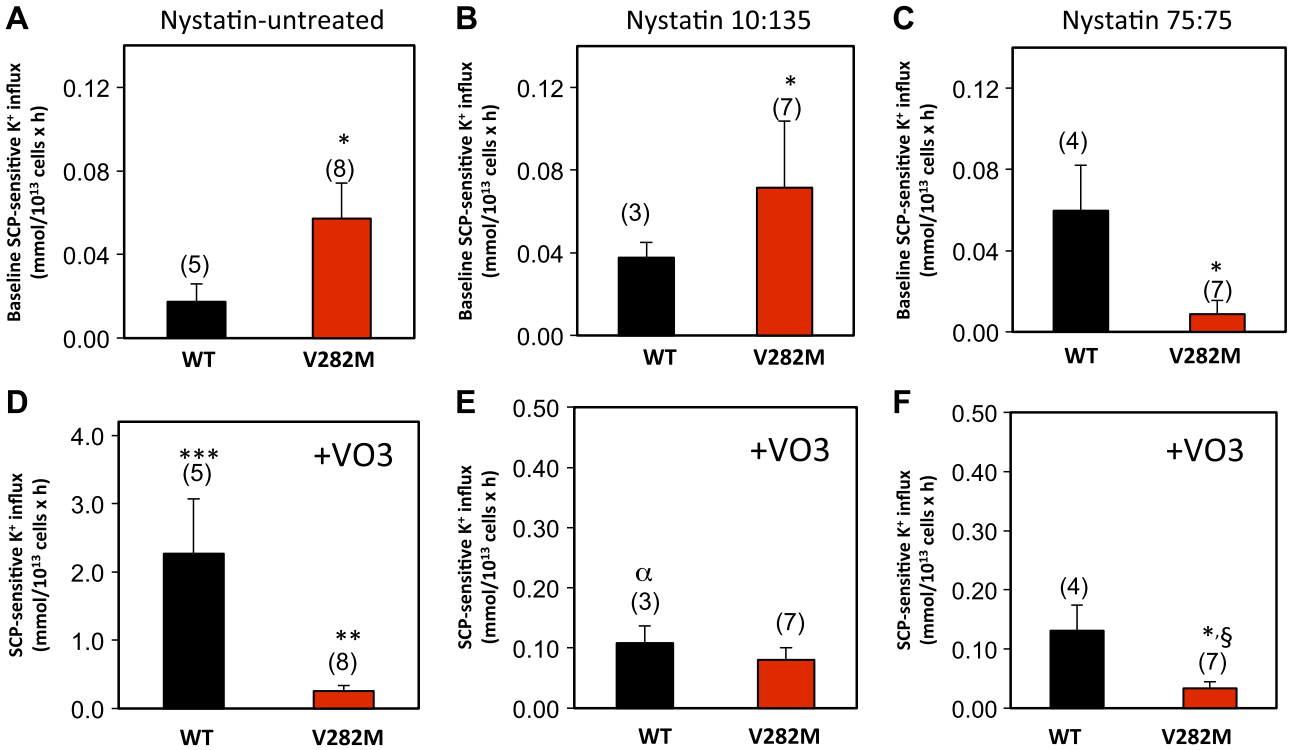

Fig. 7. Effect of nystatin-loading on senicapoc (SCP)-sensitive K^+ influx without and with orthovanadate (VO_3) stimulation in wild type (WT) and V282M hereditary xerocytosis (HX) red blood cells (RBC). Freshly isolated erythrocytes at 10% hematocrit were untreated (*A* and *B*) or nystatin-loaded in solutions containing (in mM:mM) either 10 Na:135 K (*C* and *D*) or 75 Na:75 K (*E* and *F*), as described in METHODS. Nystatin-loaded cells were then incubated for 30 min at 37°C in the absence of ouabain and bumetanide and in the absence (*A–C*) or presence of 1 mM orthovanadate (*D–F*). 200 nM SCP-sensitive ^{86}Rb influx was measured in the presence of 1.5 mM $CaCl_2$, in the absence (*A–C*) or presence of 1 mM orthovanadate (*D–F*). Values are means ± SE (*n*) experiments, each performed in triplicate, on samples from 3 different HX subjects. *$P < 0.02$ for WT vs. V282M (unpaired Mann-Whitney test); **$P = 0.0021$ for V282M ± VO_3; ***$P = 0.0002$ for WT ± VO_3; α$P < 0.033$ for WT ± VO3; §$P = 0.046$ for V282M ± VO_3 (paired Wilcoxon signed-rank test).

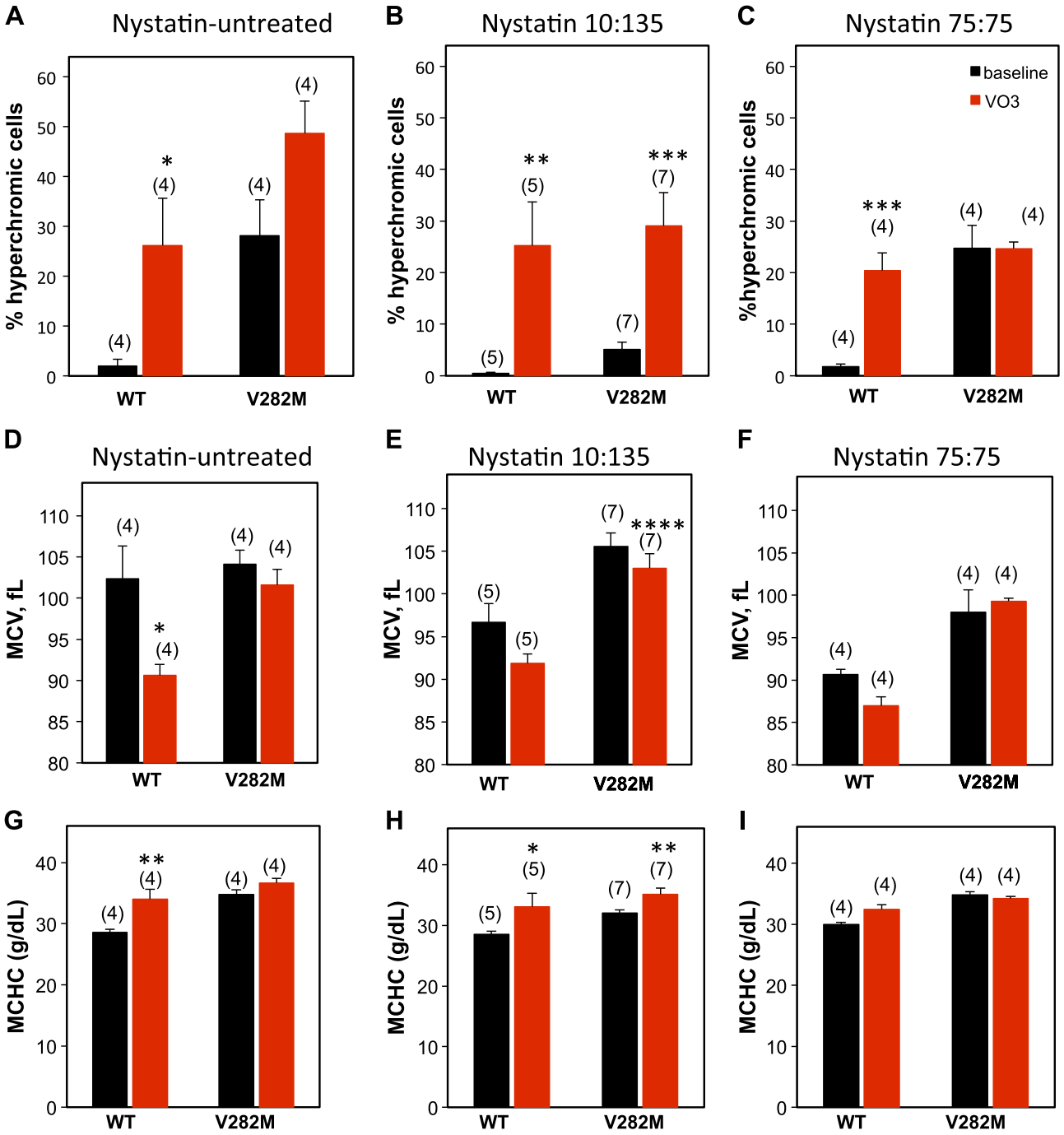

Fig. 8. Effect of orthovanadate (VO_3) on cell density and volume in Na^+- and K^+-loaded erythrocytes. Freshly isolated red cells at 10% hematocrit were untreated (*A*, *D*, and *G*) or nystatin-loaded with Na:K solutions (in mM:mM) of 10 Na:135 K (*B*, *E*, and *H*) or 75 Na:75 K (*C*, *F*, and *I*), as described in METHODS. Cells were then incubated for 30 min at 37°C in the absence (black bars) or presence of 1 mM orthovanadate (red bars) without ouabain or bumetanide and then subjected to ADVIA analysis of % hyperchromic cells (>41 g/dl Hb; *A–C*), of mean corpuscular volume (MCV; *D–F*) and mean corpuscular hemoglobin concentration (MCHC; *G–I*). Means ± SE for (*n*) experiments on samples from 3 different hereditary xerocytosis subjects. **P* = 0.02; ***P* = 0.002; ****P* = 0.0002; *****P* = 0.0001 for baseline vs. VO_3 (paired Wilcoxon signed-rank tests).

functional characterization of seven HX-associated PIEZO1 mutants expressed in inducible, stably transfected HEK-293 Flp-In T-Rex cells reported for each mutant a distinct combination of WT or prolonged inactivation kinetics, WT or reduced activation thresholds of mechanical indentation, and WT, reduced, or absent activation by sublytic hypotonic stress (22). Thus, depending on the PIEZO1 mutation and functional stimulus examined, a single HX mutant polypeptide can exhibit gain of function, loss of function, or WT function as measured by different functional assays.

Similar heterogeneity was evident in stimulated KCNN4-mediated $^{86}Rb^+$ influx into red cells from HX patients heterozygous for KCNN4 mutations as well as in red cells of those HX patients heterozygous for PIEZO1 mutations. Thus, whereas

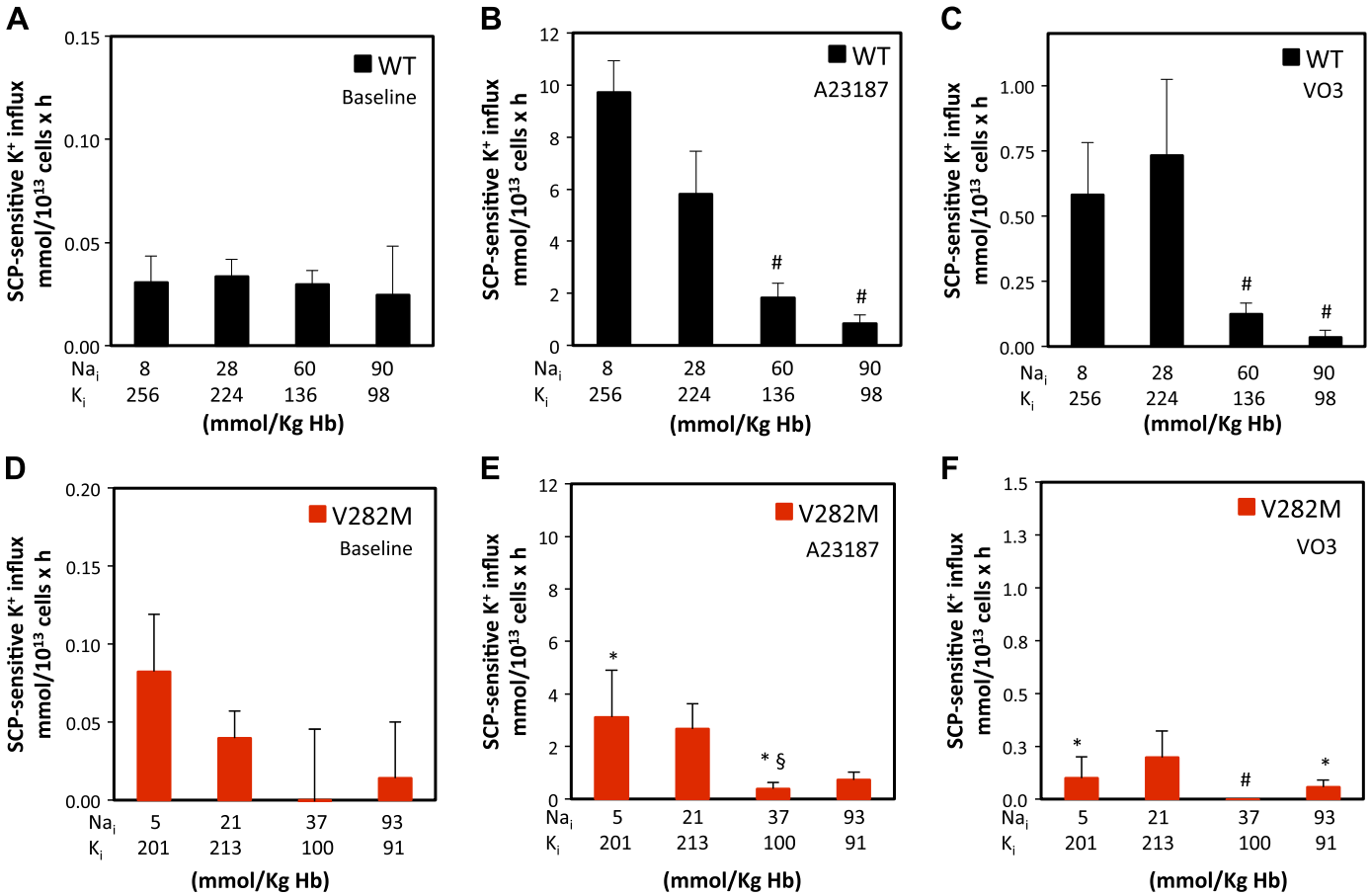

Fig. 9. Changes in intracellular cation content decrease rates of A23187-induced and orthovanadate (VO_3)-induced K^+ influx compared with baseline activity. $^{86}Rb^+$ influx was measured in wild type (WT; *A–C*) and V282M erythrocytes (*D–F*) at baseline (*A* and *D*) or stimulated by A23187 (*B* and *D*) or by orthovanadate (*C* and *F*). Cells in each condition were nystatin-pretreated in one of four solutions containing 55 mM sucrose plus (from *left* to *right* in each panel, in mM:mM) 145 Na 5:K, 140 Na 10:K, 110 Na 40:K, or 75 Na 75:K, as described in METHODS. Intracellular contents of Na (Na_i) and K (K_i) measured by atomic absorption after nystatin pretreatment in each of these four extracellular solutions are indicated along the *x*-axis of each graph. Values of senicapoc (SCP)-sensitive $^{86}Rb^+$ influx are expressed as means ± SE ($n = 3$), with each experiment performed in triplicate on samples from 2 different xerocytosis subjects subjects. *$P \leq 0.02$; §$P < 0.05$ for each V282M value vs. corresponding WT value directly above (unpaired Mann-Whitney test); #$P \leq 0.03$ vs. *leftmost* bar within each panel (Wilcoxon paired test).

KCNN4 R352H red cells exhibited orthovanadate-stimulated KCNN4 activity threefold higher than in WT cells, A23187-stimulated KCNN4 activity was equivalent in WT and mutant HX red cells (Supplemental Figs. S4*A* and S5*A*). Orthovanadate-stimulated KCNN4 activities of PIEZO1 R2456H HX red cells and of PIEZO1 V598M HX red cells resembled that of KCNN4 V282M red cells, ~20–30% that of WT cells (Supplemental Figs. S4*B* and S5*B*). In contrast, A23187-stimulated activity of HX cells of each genotype approximated that of WT cells, unlike KCNN4 V282M HX red cells (Supplemental Figs. S4*C* and S5*C*). Among the tested genotypes, only PIEZO1 R2456 HX red cells maintained a KCNN4 gain-of-function phenotype when stimulated either by orthovanadate or by A23187 (Supplemental Figs. S4*D* and S5*D*).

Measurement technique dependence of the HX loss-of-function phenotype. Unlike the KCNN4 loss-of-stimulated function phenotype exhibited by HX KCNN4 V282M red cells (Fig. 1), a cell-attached patch clamp recording of KCNN4 currents from cells of the same patients exhibited a phenotype of wild-type or increased function. A23187-stimulated, senicapoc-sensitive, cell-attached patch current was equivalent or slightly higher than for WT cells (Supplemental Fig. S3).

Whole red cell patch recordings of HX KCNN4 R352H red cells in symmetrical KCl solutions containing 1 μM Ca^{2+} revealed raw currents ~2.5-fold higher than in WT cells (42), or approximately twofold increased if normalized for the reported ~15–20% increased HX red cell surface area (48). In contrast to the V282M mutation, this gain-of-function phenotype of HX R352H red cells parallels the mutant red cells' increased stimulated senicapoc-sensitive $^{86}Rb^+$ influx (Supplemental Fig. S4). Indeed, HEK-293 cells expressing KCNN4 V282M exhibited whole cell currents only 35% higher than those expressing the wild-type protein (42), an increase compatible with A23187-stimulated, senicapoc-sensitive, cell-attached patch current on HX V282M red cells that matched or slightly exceeded that of WT cells (Supplemental Fig. S3). However, both contrasted with the 75–90% reduction in A23187- or vanadate-stimulated KCNN4-mediated $^{86}Rb^+$ influx into HX V282M red cells (Fig. 1).

Unlike whole cell patch clamp current measurements in which electrochemical K^+ gradients were identical in HX and WT cells, cell-attached patch clamp currents measured in unmodified HX red cells with lower intracellular K content reflect their reduced chemical gradient for K^+ as compared with that of wild-type cells. Moreover, the red cell membrane

in the cell-attached patch pipette is under altered tension that may mimic or exceed that of physiological red cell deformation during circulation. Such tension may account for previously observed technique-dependent differences in red cell parameters, such as those observed for anion conductance, which calculated from on-cell patch measurement was one to two orders of magnitude higher than that calculated from ion flux, voltage-sensitive dye fluorimetry, or microelectrode impedance measurements (2).

Ca^{2+} handling in the reduced flux phenotype of HX V282M red cells. The small steady-state elevation of intracellular Ca^{2+} accumulation in HX V282M cells may contribute to the increased KCNN4 baseline activity of V282M cells, but the causes of this elevated Ca^{2+} content remain unclear. KCNN4 in V282M HX red cells exhibited Ca^{2+} affinity somewhat lower than that of recombinant wild-type KCNN4 expressed in HEK-293 cells (42) but comparable with WT red cell KCNN4 (Fig. 3*C*). A23187-induced Ca^{2+} entry was not decreased but rather mildly increased in HX V282M red cells, as was steady-state Ca^{2+} accumulation, whereas orthovanadate-sensitive PMCA activity was reduced ~50% (Fig. 4). These data do not support reduced intracellular [Ca^{2+}] as a mechanism for suppressed KCNN4 stimulation in HX V282M red cells. They are compatible with possibly reduced intermediate effector activity and/or reduced effector Ca^{2+} affinity, perhaps reflecting secondary adaptations to reduced KCNN4 function.

The small steady-state elevation of intracellular Ca^{2+} accumulation in HX V282M cells may predispose to calpain activation, as occurs in response to PIEZO1 activation in vascular smooth muscle cells (31) and in activated T lymphocytes (32). Calpain can associate with PIEZO1 (35), and PIEZO1 knockdown can reduce calpain expression (36). However, treatment of RBC with a calpain inhibitor led to a previously undescribed enhancement of baseline KCNN4 activity, which in HX V282M cells was only 40% of that of WT cells (Fig. 5). The calpain inhibitor also increased A23187-stimulated KCNN4 activity in wild-type but not V282M cells. These changes likely reflect calpain stimulation of basal PMCA activity as well as calpain cleavage-mediated abrogation of calmodulin-stimulated PMCA activation (9, 38), although direct calpain action on KCNN4 or its regulators cannot be ruled out.

Red cell consequences of maximal elevation of intracellular [Ca^{2+}]. Unfractionated HX red cells share with aged normal red cells the properties of increased cell dehydration, rigidity, and susceptibility to oxidative damage. Maximal activities of both KCNN4 (55) and PMCA (30) decline monotonically with increasing age by yet-undefined mechanism(s) that may be accelerated in HX V282M red cells. The coincidence of elevated baseline KCNN4 activity and decreased stimulated KCNN4 activity in the same red cells suggests altered regulation of a stable channel population rather than changes in KCNN4 red cell surface copy number, which have varied between 10 and 125 channels/cell in older functional studies (10) and ~100–300 protomers/cell and ~2,000–4,000 protomers/white ghost in proteomic studies (12, 20).

HX V282M red cells undergo twofold accelerated ATP depletion during glucose-free incubation at 37°C (50), conditions shared by most of our measurements. However, during the 37°C influx periods of 6 min (in A23187) or 10 min (in orthovanadate), ATP levels should decline only 10–20% in WT and HX cells, declines that are further retarded by the wide-spectrum phosphatase inhibition of orthovanadate. Whether these changes might further modify ATP concentrations in delimited compartments (17, 18), decrease levels of phosphatidylinositol-bis-phosphate (required to prevent post-activation rundown for many ion channels), phosphatidylinositol-3-phosphate (52), or the already decreased levels of 2,3-diphosphoglycerate (48), or increase susceptibility to oxidative damage (51) remains unknown. Similarly unknown is how intracellular [Ca^{2+}] in WT and HX red cells interacts with these signals, with NME2-mediated histidine phosphorylation (20, 53) and other kinase and phosphatase pathways (27) shown to regulate KCNN4.

RBC exposure to A23187 increases microvesicle formation within 15 min, with prominent release within 2 h (37). Although the present experiments exposed RBC to A23187 for only 6 min, HX red cells have increased propensity to microvesiculation (50), likely accelerated by ionophore-mediated elevation of intracellular [Ca^{2+}]. Intracellular Ca^{2+} elevation also promotes phospholipid scramblase activity, exposing outer leaflet phosphatidylserine (PS) to promote erythrophagocytosis. Although surface PS exposure in the setting of elevated intracellular Ca^{2+} has not been reported higher in HX than in WT cells, red cell PS externalization promotes endothelial adhesion. In this context, comparison of HX red cells mutant in KCNN4 with those mutant in PIEZO1 might be a promising approach to investigate the predisposition to systemic thrombosis in HX secondary to PIEZO1 mutations but is not yet observed among the smaller numbers of HX patients with KCNN4 mutations (4, 39)

Regulation of stimulated KCNN4 activity by intracellular cations. We used nystatin treatment and removal to modulate intracellular monovalent cation content. We found that conferral on WT cells of an intracellular cation content resembling that of severe HX conferred on WT cells a partial (A23187) or near-complete (orthovanadate) loss-of-function phenotype comparable with that of HX V282M red cells (Fig. 6). Conversely, conferral on HX V282M red cells of an intracellular cation content resembling that of WT cells equalized orthovanadate-stimulated KCNN4 activity in WT and HX V282M cells (Fig. 7*E*). These results suggest that the intracellular balance of Na and K contributes to regulation of KCNN4 activity and to the functional changes in circulating red cells that result from heterozygosity for KCNN4 V282M.

Effect of nystatin modulation of red cell cation content on stimulated KCNN4 activity. Nystatin decreases KCNN4 activity stimulated by A23187 by ~10-fold and that stimulated by vanadate >20-fold. Nystatin is known to promote phospholipid scrambling (34), bind and sequester membrane cholesterol (16), and disrupt cholesterol-enriched lipid rafts in red cells (13, 25, 26). Incubation of cells with methyl-β-cyclodextrin (MβCD) is a standard approach to deplete cholesterol from the plasmalemmal outer leaflet and other cell cholesterol sources (29, 61), and membrane depletion or restoration/supplementation of cholesterol differentially modifies function and regulation of many ion channels and transporters (29). Cholesterol is enriched in lipid rafts in erythrocytes (47) and in other cell types, and MβCD disrupts lipid rafts. Lidocaine can disrupt erythrocyte lipid rafts, but without depleting membrane cholesterol (25, 26). Preliminary data suggest that exposure to neither MβCD (2 mM) nor lidocaine (2 or 18 mM) consistently inhibits orthovanadate-stimulated KCNN4 activity (not

shown), and neither cholesterol extraction nor lipid raft disruption likely explains the inhibitory effect of nystatin on stimulated KCNN4 activity at all modified intracellular ion contents.

Ether lipids can be important components of lipid rafts. Cholesterol sequestration by nystatin has indeed been reported to stabilize fatty acyl-CoA reductase 1 (24), likely increasing cellular levels of the ether lipid KCNN4 agonist platelet-activating factor (43). Thus, nystatin-mediated inhibition of vanadate-stimulated KCNN4 probably operates through a distinct mechanism. Indeed, functional interaction of KCNN4 and BK channels in lipid rafts of mouse parotid acinar cells was weakened after cholesterol depletion by MβCD, without reported decrease in KCNN4 activity (46). Finally, the severe reduction in KCNN4 activity produced by nystatin pretreatment itself is not intrinsically nystatin-dependent, since comparable modification of intracellular cation content by prolonged incubation in thiocyanate solutions produced comparable inhibition of KCNN4 (54).

Conclusion. We have shown that the HX-associated KCNN4 gain-of-baseline function mutation V282M exhibits a loss-of-function phenotype in patient red cells stimulated by A23187 or by orthovanadate and studied by unidirectional $^{86}Rb^+$ influx. The mechanism by which maximally (A23187-) or near-maximally (orthovanadate-) activated KCNN4 HX V282M red cells is suppressed relative to WT KCNN4 activity is not easily explained by differences in intracellular Ca^{2+}, Ca^{2+} sensitivity or senicapoc sensitivity of KCNN4 V282M, or calpain activation. However, activation state-dependent changes to the inner pore of the KCNN4 tetramer resulting from the V282M substitution likely contribute to some if not all of the complex red cell phenotype. The reduction in stimulated activity may also reflect in part the reduced intracellular K and elevated intracellular Na contents in HX RBC, but that conclusion is complicated by experimental conditions that themselves reduce KCNN4 activity.

We speculate that the phenotype of reduced stimulated KCNN4 activity in circulating HX V282M red cells subjected to measurement of $^{86}Rb^+$ influx may reflect accelerated cell aging and oxidative damage in the circulation and perhaps during erythropoiesis as well. Thus, maximally effective senicapoc treatment of HX patients heterozygous for the senicapoc-sensitive KCNN4 mutant V282M will likely require inhibition of the mutant channel throughout erythropoiesis, as well as for the subsequent circulating lifetime of the mature HX red cell. Further research will be required to understand the dual gain-of-function and loss-of-function phenotypes of KCNN4 activity in red cells of HX patients of KCNN4 genotype V282M/+.

ACKNOWLEDGMENTS

We thank the HX patients, who generously provided blood samples for this study, and Pfizer, Inc. for senicapoc.

GRANTS

Research in S. L. Alper's laboratory was supported by QUEST Diagnostics.

DISCLOSURES

J. G. Wohlgemuth and J. Morton are employees of QUEST Diagnostics. L. M. Snyder was employed by and now consults for QUEST Diagnostics. C. Brugnara is a consultant to Pfizer, Inc. and holds issued patents on clinical use of senicapoc. Research in S. L. Alper's laboratory was supported by QUEST Diagnostics. None of the other authors has any conflicts of interest, financial or otherwise, to disclose.

AUTHOR CONTRIBUTIONS

C.B., L.M.S., and S.L.A. conceived and designed research; A.R., D.H.V., B.E.S., I.A., A.I., N.M.A., E.S., M.A., and N.H. performed experiments; A.R., D.H.V., B.E.S., E.S., L.M.S., and S.L.A. analyzed data; A.R., D.H.V., I.A., A.I., N.M.A., E.S., M.A., N.H., C.B., L.M.S., and S.L.A. interpreted results of experiments; A.R., D.H.V., E.S., and S.L.A. prepared figures; A.R., D.H.V., and S.L.A. drafted manuscript; A.R., D.H.V., B.E.S., I.A., A.I., N.M.A., E.S., M.A., N.H., J.M., J.G.W., C.B., L.M.S., and S.L.A. edited and revised manuscript; A.R., D.H.V., B.E.S., I.A., A.I., N.M.A., E.S., M.A., N.H., J.M., J.G.W., C.B., L.M.S., and S.L.A. approved final version of manuscript.

REFERENCES

1. **Albuisson J, Murthy SE, Bandell M, Coste B, Louis-Dit-Picard H, Mathur J, Fénéant-Thibault M, Tertian G, de Jaureguiberry JP, Syfuss PY, Cahalan S, Garçon L, Toutain F, Simon Rohrlich P, Delaunay J, Picard V, Jeunemaitre X, Patapoutian A.** Dehydrated hereditary stomatocytosis linked to gain-of-function mutations in mechanically activated PIEZO1 ion channels. *Nat Commun* 4: 1884, 2013. [Erratum in *Nat Commun* 4: 2440, 2013.] doi:10.1038/ncomms2899.
2. **Alper SL, Vandorpe DH, Peters LL, Brugnara C.** Reduced DIDS-sensitive chloride conductance in Ae1−/− mouse erythrocytes. *Blood Cells Mol Dis* 41: 22–34, 2008. doi:10.1016/j.bcmd.2008.01.002.
3. **Andolfo I, Alper SL, De Franceschi L, Auriemma C, Russo R, De Falco L, Vallefuoco F, Esposito MR, Vandorpe DH, Shmukler BE, Narayan R, Montanaro D, D'Armiento M, Vetro A, Limongelli I, Zuffardi O, Glader BE, Schrier SL, Brugnara C, Stewart GW, Delaunay J, Iolascon A.** Multiple clinical forms of dehydrated hereditary stomatocytosis arise from mutations in PIEZO1. *Blood* 121: 3925–3935, 2013. doi:10.1182/blood-2013-02-482489.
4. **Andolfo I, Russo R, Gambale A, Iolascon A.** Hereditary stomatocytosis: an underdiagnosed condition. *Am J Hematol* 93: 107–121, 2018. doi:10.1002/ajh.24929.
5. **Andolfo I, Russo R, Manna F, Shmukler BE, Gambale A, Vitiello G, De Rosa G, Brugnara C, Alper SL, Snyder LM, Iolascon A.** Novel Gardos channel mutations linked to dehydrated hereditary stomatocytosis (xerocytosis). *Am J Hematol* 90: 921–926, 2015. doi:10.1002/ajh.24117.
6. **Andolfo I, Russo R, Rosato BE, Manna F, Gambale A, Brugnara C, Iolascon A.** Genotype-phenotype correlation and risk stratification in a cohort of 123 hereditary stomatocytosis patients. *Am J Hematol* 93: 1509–1517, 2018. doi:10.1002/ajh.25276.
7. **Archer NM, Shmukler BE, Andolfo I, Vandorpe DH, Gnanasambandam R, Higgins JM, Rivera A, Fleming MD, Sachs F, Gottlieb PA, Iolascon A, Brugnara C, Alper SL, Nathan DG.** Hereditary xerocytosis revisited. *Am J Hematol* 89: 1142–1146, 2014. doi:10.1002/ajh.23799.
8. **Bae C, Gnanasambandam R, Nicolai C, Sachs F, Gottlieb PA.** Xerocytosis is caused by mutations that alter the kinetics of the mechanosensitive channel PIEZO1. *Proc Natl Acad Sci USA* 110: E1162–E1168, 2013. doi:10.1073/pnas.1219777110.
9. **Bruce JIE.** Metabolic regulation of the PMCA: role in cell death and survival. *Cell Calcium* 69: 28–36, 2018. doi:10.1016/j.ceca.2017.06.001.
10. **Brugnara C, De Franceschi L, Alper SL.** Ca^{2+}-activated K^+ transport in erythrocytes. Comparison of binding and transport inhibition by scorpion toxins. *J Biol Chem* 268: 8760–8768, 1993.
11. **Brugnara C, Kopin AS, Bunn HF, Tosteson DC.** Regulation of cation content and cell volume in hemoglobin erythrocytes from patients with homozygous hemoglobin C disease. *J Clin Invest* 75: 1608–1617, 1985. doi:10.1172/JCI111867.
12. **Bryk AH, Wiśniewski JR.** Quantitative analysis of human red blood cell proteome. *J Proteome Res* 16: 2752–2761, 2017. doi:10.1021/acs.jproteome.7b00025.
13. **Buschiazzo J, Ialy-Radio C, Auer J, Wolf JP, Serres C, Lefèvre B, Ziyyat A.** Cholesterol depletion disorganizes oocyte membrane rafts altering mouse fertilization. *PLoS One* 8: e62919, 2013. doi:10.1371/journal.pone.0062919.
14. **Cahalan SM, Lukacs V, Ranade SS, Chien S, Bandell M, Patapoutian A.** Piezo1 links mechanical forces to red blood cell volume. *eLife* 4: e07370, 2015. doi:10.7554/eLife.07370.

15. **Caulier A, Rapetti-Mauss R, Guizouarn H, Picard V, Garçon L, Badens C.** Primary red cell hydration disorders: pathogenesis and diagnosis. *Int J Lab Hematol* 40, *Suppl* 1: 68–73, 2018. doi:10.1111/ijlh.12820.
16. **Chen CL, Liu IH, Fliesler SJ, Han X, Huang SS, Huang JS.** Cholesterol suppresses cellular TGF-beta responsiveness: implications in atherogenesis. *J Cell Sci* 120: 3509–3521, 2007. doi:10.1242/jcs.006916.
17. **Chu H, Puchulu-Campanella E, Galan JA, Tao WA, Low PS, Hoffman JF.** Identification of cytoskeletal elements enclosing the ATP pools that fuel human red blood cell membrane cation pumps. *Proc Natl Acad Sci USA* 109: 12794–12799, 2012. doi:10.1073/pnas.1209014109.
18. **Cinar E, Zhou S, DeCourcey J, Wang Y, Waugh RE, Wan J.** Piezo1 regulates mechanotransductive release of ATP from human RBCs. *Proc Natl Acad Sci USA* 112: 11783–11788, 2015. doi:10.1073/pnas.1507309112.
19. **De Franceschi L, Franco RS, Bertoldi M, Brugnara C, Matté A, Siciliano A, Wieschhaus AJ, Chishti AH, Joiner CH.** Pharmacological inhibition of calpain-1 prevents red cell dehydration and reduces Gardos channel activity in a mouse model of sickle cell disease. *FASEB J* 27: 750–759, 2013. doi:10.1096/fj.12-217836.
20. **Gautier EF, Leduc M, Cochet S, Bailly K, Lacombe C, Mohandas N, Guillonneau F, El Nemer W, Mayeux P.** Absolute proteome quantification of highly purified populations of circulating reticulocytes and mature erythrocytes. *Blood Adv* 2: 2646–2657, 2018. doi:10.1182/bloodadvances.2018023515.
21. **Glogowska E, Lezon-Geyda K, Maksimova Y, Schulz VP, Gallagher PG.** Mutations in the Gardos channel (KCNN4) are associated with hereditary xerocytosis. *Blood* 126: 1281–1284, 2015. doi:10.1182/blood-2015-07-657957.
22. **Glogowska E, Schneider ER, Maksimova Y, Schulz VP, Lezon-Geyda K, Wu J, Radhakrishnan K, Keel SB, Mahoney D, Freidmann AM, Altura RA, Gracheva EO, Bagriantsev SN, Kalfa TA, Gallagher PG.** Novel mechanisms of PIEZO1 dysfunction in hereditary xerocytosis. *Blood* 130: 1845–1856, 2017. doi:10.1182/blood-2017-05-786004.
23. **Gnanasambandam R, Rivera A, Vandorpe DH, Shmukler BE, Brugnara C, Snyder LM, Andolfo I, Iolascon A, Silveira PA, Hamerschlak N, Gottlieb P, Alper SL.** Increased red cell KCNN4 activity in sporadic hereditary xerocytosis associated with enhanced single channel pressure sensitivity of PIEZO1 mutant V598M. *Hemasphere* 2: e55, 2018. doi:10.1097/HS9.0000000000000055.
24. **Honsho M, Abe Y, Fujiki Y.** Plasmalogen biosynthesis is spatiotemporally regulated by sensing plasmalogens in the inner leaflet of plasma membranes. *Sci Rep* 7: 43936, 2017. doi:10.1038/srep43936.
25. **Kamata K, Manno S, Ozaki M, Takakuwa Y.** Functional evidence for presence of lipid rafts in erythrocyte membranes: Gsalpha in rafts is essential for signal transduction. *Am J Hematol* 83: 371–375, 2008. doi:10.1002/ajh.21126.
26. **Koshino I, Takakuwa Y.** Disruption of lipid rafts by lidocaine inhibits erythrocyte invasion by *Plasmodium falciparum*. *Exp Parasitol* 123: 381–383, 2009. doi:10.1016/j.exppara.2009.08.019.
27. **Kostova EB, Beuger BM, Klei TR, Halonen P, Lieftink C, Beijersbergen R, van den Berg TK, van Bruggen R.** Identification of signalling cascades involved in red blood cell shrinkage and vesiculation. *Biosci Rep* 35: e00187, 2015. doi:10.1042/BSR20150019.
28. **Lee CH, MacKinnon R.** Activation mechanism of a human SK-calmodulin channel complex elucidated by cryo-EM structures. *Science* 360: 508–513, 2018. doi:10.1126/science.aas9466.
29. **Levitan I, Singh DK, Rosenhouse-Dantsker A.** Cholesterol binding to ion channels. *Front Physiol* 5: 65, 2014. doi:10.3389/fphys.2014.00065.
30. **Lew VL, Daw N, Etzion Z, Tiffert T, Muoma A, Vanagas L, Bookchin RM.** Effects of age-dependent membrane transport changes on the homeostasis of senescent human red blood cells. *Blood* 110: 1334–1342, 2007. doi:10.1182/blood-2006-11-057232.
31. **Li J, Hou B, Tumova S, Muraki K, Bruns A, Ludlow MJ, Sedo A, Hyman AJ, McKeown L, Young RS, Yuldasheva NY, Majeed Y, Wilson LA, Rode B, Bailey MA, Kim HR, Fu Z, Carter DA, Bilton J, Imrie H, Ajuh P, Dear TN, Cubbon RM, Kearney MT, Prasad RK, Evans PC, Ainscough JF, Beech DJ.** Piezo1 integration of vascular architecture with physiological force. *Nature* 515: 279–282, 2014. doi:10.1038/nature13701.
32. **Liu CSC, Raychaudhuri D, Paul B, Chakrabarty Y, Ghosh AR, Rahaman O, Talukdar A, Ganguly D.** Cutting edge: Piezo1 mechanosensors optimize human t cell activation. *J Immunol* 200: 1255–1260, 2018. doi:10.4049/jimmunol.1701118.
33. **Ma S, Cahalan S, LaMonte G, Grubaugh ND, Zeng W, Murthy SE, Paytas E, Gamini R, Lukacs V, Whitwam T, Loud M, Lohia R, Berry L, Khan SM, Janse CJ, Bandell M, Schmedt C, Wengelnik K, Su AI, Honore E, Winzeler EA, Andersen KG, Patapoutian A.** Common PIEZO1 allele in African populations causes RBC dehydration and attenuates plasmodium infection. *Cell* 173: 443–455.e12, 2018. doi:10.1016/j.cell.2018.02.047.
34. **Malik A, Bissinger R, Jilani K, Lang F.** Stimulation of erythrocyte cell membrane scrambling by nystatin. *Basic Clin Pharmacol Toxicol* 116: 47–52, 2015. doi:10.1111/bcpt.12279.
35. **McHugh BJ, Buttery R, Lad Y, Banks S, Haslett C, Sethi T.** Integrin activation by Fam38A uses a novel mechanism of R-Ras targeting to the endoplasmic reticulum. *J Cell Sci* 123: 51–61, 2010. doi:10.1242/jcs.056424.
36. **McHugh BJ, Murdoch A, Haslett C, Sethi T.** Loss of the integrin-activating transmembrane protein Fam38A (Piezo1) promotes a switch to a reduced integrin-dependent mode of cell migration. *PLoS One* 7: e40346, 2012. doi:10.1371/journal.pone.0040346.
37. **Nguyen DB, Ly TB, Wesseling MC, Hittinger M, Torge A, Devitt A, Perrie Y, Bernhardt I.** Characterization of microvesicles released from human red blood cells. *Cell Physiol Biochem* 38: 1085–1099, 2016. doi:10.1159/000443059.
38. **Pengpanichpakdee N, Thadtapong T, Auparakkitanon S, Wilairat P.** Plasma membrane Ca^{2+}-ATPase sulfhydryl modifications: implication for oxidized red cell. *Southeast Asian J Trop Med Public Health* 43: 1252–1257, 2012.
39. **Picard V, Guitton C, Thuret I, Rose C, Bendelac L, Ghazal K, Aguilar-Martinez P, Badens C, Barro C, Bénéteau C, Berger C, Cathébras P, Deconinck E, Delaunay J, Durand JM, Firah N, Galactéros F, Godeau B, Jaïs X, de Jaureguiberry JP, Le Stradic C, Lifermann F, Maffre R, Morin G, Perrin J, Proulle V, Ruivard M, Toutain F, Lahary A, Garçon L.** Clinical and biological features in PIEZO1-hereditary xerocytosis and Gardos-channelopathy: a retrospective series of 126 patients. *Haematologica*. In press. doi:10.3324/haematol.2018.205328.
40. **Raftos JE, Edgley A, Bookchin RM, Etzion Z, Lew VL, Tiffert T.** Normal Ca^{2+} extrusion by the Ca^{2+} pump of intact red blood cells exposed to high glucose concentrations. *Am J Physiol Cell Physiol* 280: C1449–C1454, 2001. doi:10.1152/ajpcell.2001.280.6.C1449.
41. **Rapetti-Mauss R, Lacoste C, Picard V, Guitton C, Lombard E, Loosveld M, Nivaggioni V, Dasilva N, Salgado D, Desvignes JP, Béroud C, Viout P, Bernard M, Soriani O, Vinti H, Lacroze V, Feneant-Thibault M, Thuret I, Guizouarn H, Badens C.** A mutation in the Gardos channel is associated with hereditary xerocytosis. *Blood* 126: 1273–1280, 2015. doi:10.1182/blood-2015-04-642496.
42. **Rapetti-Mauss R, Soriani O, Vinti H, Badens C, Guizouarn H.** Senicapoc: a potent candidate for the treatment of a subset of hereditary xerocytosis caused by mutations in the Gardos channel. *Haematologica* 101: e431–e435, 2016. doi:10.3324/haematol.2016.149104.
43. **Rivera A, Jarolim P, Brugnara C.** Modulation of Gardos channel activity by cytokines in sickle erythrocytes. *Blood* 99: 357–363, 2002. doi:10.1182/blood.V99.1.357.
44. **Rivera A, Vandorpe DH, Shmukler BE, Gallagher DR, Fikry CC, Kuypers FA, Brugnara C, Snyder LM, Alper SL.** Erythrocytes from hereditary xerocytosis patients heterozygous for KCNN4 V282M exhibit increased spontaneous Gardos channel-like activity inhibited by senicapoc. *Am J Hematol* 92: E108–E110, 2017. doi:10.1002/ajh.24716.
45. **Rivera A, Zee RY, Alper SL, Peters LL, Brugnara C.** Strain-specific variations in cation content and transport in mouse erythrocytes. *Physiol Genomics* 45: 343–350, 2013. doi:10.1152/physiolgenomics.00143.2012.
46. **Romanenko VG, Roser KS, Melvin JE, Begenisich T.** The role of cell cholesterol and the cytoskeleton in the interaction between IK1 and maxi-K channels. *Am J Physiol Cell Physiol* 296: C878–C888, 2009. doi:10.1152/ajpcell.00438.2008.
47. **Salzer U, Prohaska R.** Stomatin, flotillin-1, and flotillin-2 are major integral proteins of erythrocyte lipid rafts. *Blood* 97: 1141–1143, 2001. doi:10.1182/blood.V97.4.1141.
48. **Sauberman N, Fairbanks G, Lutz HU, Fortier NL, Snyder LM.** Altered red blood cell surface area in hereditary xerocytosis. *Clin Chim Acta* 114: 149–161, 1981. doi:10.1016/0009-8981(81)90388-0.
49. **Shmukler BE, Vandorpe DH, Rivera A, Auerbach M, Brugnara C, Alper SL.** Dehydrated stomatocytic anemia due to the heterozygous mutation R2456H in the mechanosensitive cation channel PIEZO1: a case

report. *Blood Cells Mol Dis* 52: 53–54, 2014. doi:10.1016/j.bcmd.2013.07.015.

50. **Snyder LM, Lutz HU, Sauberman N, Jacobs J, Fortier NL.** Fragmentation and myelin formation in hereditary xerocytosis and other hemolytic anemias. *Blood* 52: 750–761, 1978.
51. **Snyder LM, Sauberman N, Condara H, Dolan J, Jacobs J, Szymanski I, Fortier NL.** Red cell membrane response to hydrogen peroxide-sensitivity in hereditary xerocytosis and in other abnormal red cells. *Br J Haematol* 48: 435–444, 1981. doi:10.1111/j.1365-2141.1981.tb02735.x.
52. **Srivastava S, Choudhury P, Li Z, Liu G, Nadkarni V, Ko K, Coetzee WA, Skolnik EY.** Phosphatidylinositol 3-phosphate indirectly activates KCa3.1 via 14 amino acids in the carboxy terminus of KCa3.1. *Mol Biol Cell* 17: 146–154, 2006. doi:10.1091/mbc.e05-08-0763.
53. **Srivastava S, Li Z, Ko K, Choudhury P, Albaqumi M, Johnson AK, Yan Y, Backer JM, Unutmaz D, Coetzee WA, Skolnik EY.** Histidine phosphorylation of the potassium channel KCa3.1 by nucleoside diphosphate kinase B is required for activation of KCa3.1 and CD4 T cells. *Mol Cell* 24: 665–675, 2006. doi:10.1016/j.molcel.2006.11.012.
54. **Stampe P, Vestergaard-Bogind B.** Ca^{2+}-activated K^+ conductance of the human red cell membrane: voltage-dependent Na^+ block of outward-going currents. *J Membr Biol* 112: 9–14, 1989. doi:10.1007/BF01871159.
55. **Tiffert T, Daw N, Etzion Z, Bookchin RM, Lew VL.** Age decline in the activity of the Ca^{2+}-sensitive K^+ channel of human red blood cells. *J Gen Physiol* 129: 429–436, 2007. doi:10.1085/jgp.200709766.
56. **Utsugisawa TIT, Aoki T, Okamoto Y, Kawakami T, Ogura H, Kanno H.** The flow cytometric osmotic fragility test is an effective screening mthod for dehydrated hereditary stomatocytosis. *Blood* 132: 929, 2017.
57. **Vandorpe DH, Xu C, Shmukler BE, Otterbein LE, Trudel M, Sachs F, Gottlieb PA, Brugnara C, Alper SL.** Hypoxia activates a Ca^{2+}-permeable cation conductance sensitive to carbon monoxide and to GsMTx-4 in human and mouse sickle erythrocytes. *PLoS One* 5: e8732, 2010. doi:10.1371/journal.pone.0008732.
58. **Wieschhaus A, Khan A, Zaidi A, Rogalin H, Hanada T, Liu F, De Franceschi L, Brugnara C, Rivera A, Chishti AH.** Calpain-1 knockout reveals broad effects on erythrocyte deformability and physiology. *Biochem J* 448: 141–152, 2012. doi:10.1042/BJ20121008.
59. **Yingst DR, Hoffman JF.** Ca-induced K transport in human red blood cell ghosts containing arsenazo III. Transmembrane interactions of Na, K, and Ca and the relationship to the functioning Na-K pump. *J Gen Physiol* 83: 19–45, 1984. doi:10.1085/jgp.83.1.19.
60. **Zarychanski R, Schulz VP, Houston BL, Maksimova Y, Houston DS, Smith B, Rinehart J, Gallagher PG.** Mutations in the mechanotransduction protein PIEZO1 are associated with hereditary xerocytosis. *Blood* 120: 1908–1915, 2012. doi:10.1182/blood-2012-04-422253.
61. **Zidovetzki R, Levitan I.** Use of cyclodextrins to manipulate plasma membrane cholesterol content: evidence, misconceptions and control strategies. *Biochim Biophys Acta* 1768: 1311–1324, 2007. doi:10.1016/j.bbamem.2007.03.026.